Pricing Beyond Insurance: Capital Markets and Emerging Risks

Marcel Freyschmidt[*,†]

Emerging risks like climate change and cyber threats are reshaping traditional risk-sharing between policyholders and (re)insurers, with capital markets underwriting these risks through catastrophe bonds and cyber bonds. These instruments, driven by tail risks and offering high returns and portfolio diversification, are challenging to explain using traditional asset pricing models. This study introduces a pricing model based on option pricing theory to address this gap, demonstrating its effectiveness using real-world cyber data. The model reveals a unique probability distortion towards tail risk, even in incomplete markets. This distortion is rooted in prospect theory and offers new insights into asset pricing. The findings provide valuable guidance for investors, regulators, and researchers dealing with the complexities of tail risks.

Keywords: Emerging Risk, NatCat Risk, Cyber Risk, Cat Bond, Cyber Bond, Option Pricing, Jump Processes, Tail Risk, Prospect Theory

---

[*] marcel.freyschmidt@unisg.ch; Girtannerstrasse 6, CH-9010 St.Gallen; Phone +41 71 224 7974.

[†] I thank the participants of the American Risk and Insurance Association Annual Meeting 2024, the PhD Workshop Gais 2024, the Research Seminar of the Institute of Insurance Economics at University of St. Gallen 2024, the Modern Finance Conference 2024, and the Swiss Finance Institute Academic Job Market Workshop, Piotr Mielus, Hato Schmeiser, Alexander Braun, Markus Huggenberger, and especially George Zanjani and Martin Eling for their valuable comments.

1 Introduction

The increasing frequency and severity of natural disasters driven by climate change have expanded the scope of private risk-sharing beyond traditional property and casualty insurance. Additionally, the rise of cyber threats due to global networking and digitalization has further broadened this scope, challenging the conventional policyholder-insurer relationship. Today, insurance-linked securities such as catastrophe bonds (cat bonds) and cyber bonds actively integrate capital markets into the risk-sharing process. (Re)insurers or brokers initially underwrite tail risks from policyholders. Subsequently, they transfer these risks to the capital markets, effectively becoming bondholders to seek protection through the capital markets in case of a triggering event. These risks are largely uncorrelated with capital market risks, making them attractive for investment due to their high returns and diversification potential (Cummins and Weiss, 2009). However, extreme losses push the limits of the capital market and underscore the necessity for alternative solutions, such as government involvement, as illustrated by the Covid-19 pandemic (e.g., Gründl et al., 2021; Braun et al., 2023). With the rise of climate and cyber risks, along with the recent Covid-19 pandemic, the presence of jump risks and their correlation with macroeconomic fundamentals has become increasingly important. Understanding and replicating the returns of cat bonds – a key instrument for protection against these risks and which are almost entirely composed of uncorrelated tail risks – remains an unsolved puzzle. Traditional asset pricing models, including factor models and consumption-based models, typically explain only a small portion of the risk premium (e.g., Braun et al., 2019a). Moreover, the availability of high-frequency natural catastrophe risk data is limited, and long-term data is scarce, especially for relatively new markets like cyber bonds. In the case of pandemics, data is virtually non-existent. The lack of explanatory power in traditional asset pricing models is not unique to the cat bond market. For instance, corporate bond markets, where downside risks are known pricing factors, also reveal the limitations of traditional pricing models (e.g., Bai et al., 2019; Dickerson et al., 2023).

The inability of traditional models to explain the returns on cat bonds poses an issue for effective pricing and risk management in a rapidly growing risk transfer market. This paper addresses this gap by introducing a comprehensive model for pricing risk transfer instruments, focusing on cat bonds and cyber bonds. Therefore, the study bridges two key domains: actuarial science, particularly in catastrophe risk modeling and pricing, and financial economics, with an emphasis on tail risk transfer mechanisms and capital market integration through instruments like cat bonds. By integrating this dual perspective, the model leverages option pricing frameworks to value different risk categories, demonstrating its applicability to capital market instruments like cat bonds or cyber bonds. This choice is particularly suitable as options are themselves hedging instruments. Unlike traditional insurance models, this approach incorporates market environment, correlations, jump risks, and higher-order factors, creating a unified framework for pricing various risks.

In insurance, catastrophic risks are often modeled using compounded Poisson processes (e.g., Bowers et al., 1986; Lee and Yu, 2002; Ma and Ma, 2013), as are in finance, asset, and option pricing models that incorporate jump risks using these widely used processes (e.g., Bates, 1996; Andersen et al., 2002; Kou, 2002; Eraker, 2004). Additionally, frictional costs are recognized as a contributing factor to high catastrophe markups (e.g., Zanjani,

2002) and explain return variations in financial markets (e.g., Luttmer, 1996; De Roon and Szymanowska, 2012; Ai and Bhandari, 2021). Grounded in the insurance model by Doherty and Garven (1986), which includes shareholders and policyholders and accounts for frictional costs, this paper also draws from option pricing models, such as the one by Margrabe (1978), which focuses on the exchange dynamics of two risky assets, and the model by Merton (1976), which incorporates jump risks. The closed-form solution provided by Cheang and Chiarella (2011) effectively integrates these models. The stochastic structure relies on a compounded Poisson jump process, consisting of a Poisson process for jump occurrences, with a jump size component. At the heart of the model is the measure transformation of the jump process from $\mathbb{P}$ to $\mathbb{Q}$, rooted in actuarial principles of probability distortion, as proposed by Esscher (1932), Gerber and Shiu (1994), and Wang (2000). In line with the financial literature, this distortion reflects investors' fear of tail risks (Bollerslev and Todorov, 2011) or an extreme aversion to significant losses and negative skewness (Pan, 2002). While the distortion is unique in simpler market settings, it becomes complex in incomplete markets, highlighting the challenge of identifying a single $\mathbb{Q}$ measure.

The paper demonstrates the practical application of the new methodology using real loss estimates across different risk categories, such as classical P&C risks and hurricane risks, calibrating model parameters with market data. Applying this approach to the cat bond market enables a focused examination of how capital markets perceive tail risk, given that cat bonds largely consist of uncorrelated tail risk. A core element of the analysis is the use of unique cyber data, providing the closest real-world calibration to date. The findings reveal that, despite market incompleteness and infinite choices for $\mathbb{Q}$, the probability distortion toward tail risks is unique. Gao et al. (2019) describe this as tail risk concerns, reflecting investors' subjective ex-ante beliefs, a behavior predicted by prospect theory (Barberis, 2013). As shown by Barberis and Huang (2008), prospect theory anticipates that skewness in a security's return distribution – even idiosyncratic skewness unrelated to the market, as in the case of cat bonds – will be priced, a feature not captured by traditional models. This paper's measure thus quantifies a distinctive pricing structure that extends beyond conventional models, serving as a unique metric of risk aversion within the framework of prospect theory.

The main contribution of this paper is twofold: First, it introduces a comprehensive model for pricing risk transfer instruments across insurance and capital markets, adding a new dimension to risk pricing theory. For non-jump risks, the approach incorporates the market environment and higher-order factors typically absent from classical insurance pricing models. For jump risks, particularly those transferred to the capital market, this paper is the first to price these instruments. The analysis has several key advantages: (1) The use of unique industrial cyber data enables a precise, real-world examination of pricing in the cyber bond market. (2) The current homogeneous market presents a rare opportunity to determine the tail risk parameter using a single dataset – an opportunity that may diminish as bond structures diversify. (3) By focusing exclusively on bonds with pure tail risk, the analysis avoids interference from other factors that could influence returns. Second, the paper demonstrates the existence of a unique $\mathbb{Q}$ for tail risks in incomplete markets rooted in established behavioral theories. The initial findings suggest that returns are composed of three main components: frictional costs, a traditional beta risk premium, and tail risk premium based on prospect theory under $\mathbb{Q}$. This aversion quantification via the mass transformation in the jump can be applied to various markets, including the S&P 500 index and options markets.

These findings are important for both investors and policymakers as they provide a deeper understanding of tail risk pricing and its implications in markets exposed to extreme events. For investors, the model offers a robust framework to assess the risk-return dynamics of high-yield, low-correlation instruments like cat bonds and cyber bonds, allowing for more informed investment decisions that align with their risk tolerance and diversification goals. For policymakers, this research shows how extreme risks are transferred and priced in capital markets, helping to inform regulatory strategies and public-private partnerships aimed at bolstering market resilience. By bridging insights from both finance and insurance, this study supports a more integrated approach to managing and pricing emerging risks, supporting stability in the face of growing climate, cyber, and pandemic-related threats. For researchers, the framework offers a foundation for further studies in risk transfer pricing and offers a new understanding of capital market returns.

This paper extends the literature on catastrophe pricing in insurance, as well as tail risk pricing and investor behavior in finance. Zanjani (2002) highlights the limitations of traditional asset pricing models in measuring catastrophic markups in insurance pricing, asserting that a significant portion of these markups stems from frictional costs and high capital requirements – an assumption that remains valid today. Similarly, Lane and Mahul (2008) emphasize that factors such as the capital market cycle and the transaction's risk profile play important roles in pricing, with market diversification also being factored in. While these elements contribute to the overall explanation, they still can explain substantial parts of risk pricing. The most closely related cat bond pricing models to this paper can be traced back to those developed by Lee and Yu (2002) and Ma and Ma (2013), which utilize contingent claim models based on compounded Poisson processes. However, these models differ from the approach presented in this paper in three significant ways: First, they focus exclusively on cat bonds without addressing the pricing of diverse risks. Second, they do not offer a closed-form solution. Third, and most critically, they follow the Merton (1976) model, incorporating unpriced risk, which limits their ability to explain observed market prices. In financial markets, jump risks are critical for pricing in high-volatility environments, such as oil and electricity markets, as well as during stock market crashes (e.g., Eraker et al., 2003; Caldana and Fusai, 2013). Research on tail risks and risk premiums is extensive; for instance, Harvey and Siddique (2000), Bollerslev and Todorov (2011), and Kelly and Jiang (2014) demonstrate that a significant portion of observed risk premiums compensates for rare events. Andersen et al. (2020) show that compensation for negative jump risk is a primary driver of premiums in international options markets. Furthermore, Ai and Bhandari (2021) illustrate that exposure to downside tail risk results in quantitatively large and volatile risk premiums. As these returns cannot be explained by classical asset pricing models, the works of Barberis and Huang (2008) and Barberis et al. (2021) link these tail returns to prospect theory, which also forms the theoretical foundation of this paper.

This paper is structured as follows. Section 2 introduces the model, defines its boundaries, and describes its connection to existing pricing models. Section 3 demonstrates the market application. Section 4 shows the real-word calibration of $\mathbb{Q}$. Section 5 discusses the results and limitations. Section 6 concludes.

2 Model

2.1 Risk Categories

To determine which risks adhere to the traditional policyholder-(re)insurance framework and at what point capital market involvement or government backstops are required, it is essential to categorize them. This paper defines four risk categories based on the framework proposed by Cummins (2006) and further specified by Braun et al. (2023), assigning each a mathematical component. It is important to note that these categories are not mutually exclusive. For instance, cyber risk may be managed through traditional (re)insurance, transferred to the capital markets, and involve discussions of government backstops, depending on the severity (e.g., Kasper et al., 2024).

The first category, called *locally insurable risk*, pertains to independent risks characterized by moderate standard deviations per risk and a substantial number of policies, such as the US market for personal automobile insurance. Local insurers can effectively cover these losses. The second category is *globally insurable risk*, which encompasses risks that are locally dependent but globally independent, such as tornadoes in the American Midwest versus Australia. Local insurers may lack the capacity to cover such losses, but global reinsurers can. Consequently, these risks are diversifiable on a global scale through reinsurance. Locally insurable risks follow a straightforward framework based on the law of large numbers, assuming independence of losses within a loss portfolio. However, this independence does not hold when analyzing globally insurable risks from a local perspective. On a global scale, these risks exhibit no interdependence, allowing the creation of a loss portfolio of independent losses. Thus, while there may be variations in the sizes of loss portfolios, local and global insurable risks are mathematically comparable and can be modeled using right-skewed and independent random variables (e.g., Eling, 2012). The third category is *globally diversifiable risk*, referring to risks with low frequency and high severity. A recent example would be the CrowdStrike outage or Hurricane Milton. The capacity of insurance and reinsurance companies may prove insufficient to cover such events, but these risks can be globally diversified through capital markets. The last category, called *globally undiversifiable risk*, describes risks of such severity that they may resist global diversification, even through capital markets, for example, the Covid-19 pandemic. While global securities markets might absorb a fraction of such a loss, complete diversification of the full loss is unlikely, and government aid is likely needed. Globally diversifiable and globally undiversifiable risks share characteristics of low frequency and high severity, with heavy tail events significantly influencing these risk profiles. They follow a structure of jump processes, such as a compounded Poisson process (e.g., Merton, 1976), which is a common assumption in the actuarial literature (e.g., Bowers et al., 1986; Lee and Yu, 2002; Jaimungal and Wang, 2006). A key distinction lies in the impact of globally undiversifiable risks, which can directly influence macroeconomic fundamentals and trigger worldwide economic shocks, as seen with the Covid-19 pandemic (e.g., Gründl et al., 2021; Braun et al., 2023). Mathematically, globally diversifiable risks are those with jumps and jump sizes uncorrelated to the capital market or, more broadly, the global economy. In contrast, globally undiversifiable risks involve a joint jump process with correlated jump sizes.[1]

2.2 Shareholder and Policyholder

Inspired by Doherty and Garven (1986), a single-period model is considered. In $t = 0$ shareholders contribute equity S_0 and policyholders pay premiums P to cover the stochastic loss $\bar{L}$. The shareholders' opening cash flow is:

$$Y_0 = S_0 + P,$$

where the cash flow is invested at a risky rate $\bar{r}$. The terminal cash flow is:

$$\bar{Y}_1 = (1 + \bar{r})\big(S_0 + P\big).$$

At the end of the period, the policyholders claim $\bar{L} \geq 0$, and the government (or other organizations such as supervisory authorities) claims frictional cost of capital $\bar{T}_1 \geq 0$. The policyholders receive the payment:

$$\bar{H}_1 = min(\bar{L}, \bar{Y}_1) = \bar{Y}_1 - max(\bar{Y}_1 - \bar{L}, 0),$$

and the additional frictional cost of capital are:

$$\bar{T}_1 = max(\tau(\bar{Y}_1 - \bar{L}), 0),$$

where τ is the rate for the frictional costs. This model, therefore, differs significantly from the underlying concept of Doherty and Garven (1986). While in their model τ represents the tax rate on income and is dependent on the premium, here τ encompasses costs related to agency, supervision, liquidity and other expenses (Froot and Stein, 1998, Zanjani, 2002). The approach followed here aligns with the logic of Zanjani (2002), who identified these costs as a key factor driving (catastrophic) insurance prices.

Both claims exhibit cash flows analogous to a European call option,[2] so the present values are:

$$\begin{aligned} H_0 &= V(\bar{Y}_1) - C(\bar{Y}_1; \bar{L}), \\ T_0 &= \tau C(\bar{Y}_1; \bar{L}), \end{aligned}$$

where $V(\cdot)$ is a present valuation operator and $C(A; B)$ is the current market value of a European call option with a terminal value A and exercise price B.

---

[1] Despite the economic coherence and comprehensiveness of these categories, which encompass all main private and public risk bearers, it is essential to address the underlying mathematical nuances. Cummins falls short in today's market environment, particularly for the last two categories. Cummins defines the last two categories of catastrophes as events that violate the principal insurability condition and may be globally diversifiable through capital markets if other conditions are satisfied. However, he does not specify mathematical concepts for these categories, unlike the first two.

[2] The cash flow of a European call option is $CF_{call} = max(A - B, 0)$ with terminal value A and exercise price B.

The present market value of the shareholders' return on equity, V_e, is the difference between the market value of the portfolio, $V(\bar{Y}_1)$, on the one side, and the present value of the policyholders' claims and the present value of the frictional costs on the other side:

$$V_e = V(\bar{Y}_1) - H_0 - T_0 = C(\bar{Y}_1; \bar{L}) - \tau C(\bar{Y}_1; \bar{L}).$$

In summary, shareholders hold a long position in a call option on the pre-frictional terminal value of the asset portfolio and a short position in a call option on the frictional costs of that portfolio.

Risk transfer prices are determined to yield a fair return to shareholders, achieved when the current market value of the equity claim equals the initial investment. As $\bar{Y}_1$ and Y_0 are functions contingent on P, the objective is to identify the premium P^* that satisfies:

$$V_e = C(\bar{Y}_1(P^*); \bar{L}) - \tau C(\bar{Y}_1(P^*); \bar{L}) = S_0. \tag{1}$$

Calculating P^* necessitates employing a suitable option-pricing framework. Given the stochastic nature of the exercise price, conventional models like Black and Scholes (1973) are impractical. Doherty and Garven (1986) establish pricing relationships within the discrete-time, risk-neutral-valuation framework of Rubinstein (1976), focusing on two special cases with (log-)normally distributed stochastic components.[3] The option pricing model used in this study is rooted in the work from Merton (1976) and Margrabe (1978), accounting for jump risks. Therefore, the model accounts for tail risks, which are becoming increasingly important in a globally expanding world with more severe climate and cyber risks. The model presented in this section will be referred to as the OM (option model) throughout the rest of the paper.

Note, globally diversifiable risk and globally undiversifiable risk refers to the type of risk that is transferred to the capital market due to the amount of capital required which cannot be adequately provided by (re)insurers alone. This transfer of risk to the capital market typically involves the issuance of a cat bond. Shareholders of the bond pay a principal amount S_0 to a trust account at time $t = 0$. In return, at time $t = 1$, they receive the risk-free rate r_f earned from the trust account, a coupon payment C, and the principal, and need to pay the incurred losses (and any additional expenses). Therefore, the terminal cash flow for the shareholder is given by:

$$\bar{Y}_1 = (1 + r_f)S_0 + C,$$

whereby $\bar{H}_1$ and $\bar{T}_1$ remain the same. To ensure that the initial cash flow for shareholders remains consistent throughout the model proposed here, the initial cash flow is:

$$Y_0 = S_0 + \frac{C}{1+\omega}.$$

Here, ω represents a risk-adjusted discount rate, and $P = \frac{C}{1+\omega}$ denotes the present value premium paid by the policyholder (Braun et al., 2023).

---

[3] Distribution assumptions like the normal distribution prove inadequate, as highlighted by Eling (2012).

2.3 Pricing the Option

Consider tradable assets X_1 and X_2 under a probability measure $\mathbb{P}$. Extending the option price formula from Black and Scholes (1973), Margrabe (1978) formulated a model allowing the exchange of two risky assets. It is assumed that all returns come from capital gains and that no dividends are distributed.[4] The dynamics for each asset are expressed as:

$$\frac{dX_i}{X_i} = \mu_i dt + \sigma_i dW_{i,t} \qquad i \in \{1, 2\},$$

where μ_i is the instantaneous expected return per unit time, σ_i is the instantaneous volatility per unit time and both assets follow a Brownian motion $dW_{i,t}$ with correlation ρ. This setting has the closed-form solution:

$$\begin{aligned} C(X_1, X_2) &= X_1\Phi(d_1) - X_2\Phi(d_2), \\ \text{with} \quad d_1 &= \frac{ln(\frac{X_1}{X_2}) + \frac{1}{2}\sigma^2(T-t)}{\sigma\sqrt{T-t}}, \\ d_2 &= d_1 - \sigma\sqrt{T-t}. \end{aligned}$$

$T - t$ represents the difference between the exercise period and the present period, $\Phi(\cdot)$ is the cumulative standard normal density function, and $\sigma^2 = \sigma_1^2 - 2\sigma_1\sigma_2\rho + \sigma_2^2$.[5]

Globally diversifiable and globally undiversifiable risks are characterized by low frequency and high severity events that fall beyond the scope of Margrabe (1978). The emergence of globally undiversifiable risk is inherently tied to economic fundamentals, indicating that not only does the loss portfolio but also the asset side exhibit a correlated downside risk. Modeling tail risk involves incorporating jump processes, aligning with the conceptual framework established in Merton (1976). Unlike Margrabe, Merton's model does not consider the exchange of two risky assets but follows the methodology of Black and Scholes (1973). Consequently, a synthesis of both approaches becomes essential in this context.

Let N_t be a Poisson process with a constant arrival rate of jumps λ, shared by both assets. The bivariate process $\boldsymbol{Y} = (Y_1, Y_2)^T$ represents the jump sizes, taking values $\boldsymbol{y} = (y_1, y_2)^T \in \mathbb{R}^2$. The jump sizes Y_n are independently and identically distributed as multivariate normal $\mathcal{N}(\boldsymbol{\alpha}, \Sigma_{\boldsymbol{Y}})$, where $\boldsymbol{\alpha} = (\alpha_1, \alpha_2)^T$, and the covariance matrix $\Sigma_{\boldsymbol{Y}}$ is given by:

$$\Sigma_{\boldsymbol{Y}} = \begin{pmatrix} \delta_1^2 & \rho_{\boldsymbol{Y}}\delta_1\delta_2 \\ \rho_{\boldsymbol{Y}}\delta_1\delta_2 & \delta_2^2 \end{pmatrix},$$

with $\rho_{\boldsymbol{Y}}$ representing the correlation between the jump sizes Y_1 and Y_2. The expected proportional common jump sizes are expressed as:

$$\kappa_i = \mathbb{E}_{\mathbb{P}}[\exp(Y_i) - 1)] = \int_{\mathbb{R}} [\exp(Y_i) - 1] m_{\mathbb{P}}(dy_i) \qquad i \in \{1, 2\},$$

---

[4] The examination of dividend payout, as discussed in papers such as Cheang and Chiarella (2011), can be easily incorporated into the model. However, since it does not constitute a central core here, it is omitted to prevent additional complexity, but discussed in Appendix A.2.

[5] For $\sigma^2 = \sigma_1^2$ and $\sigma_2 = 0$, the formula from Black and Scholes (1973) is obtained.

where $m_{\mathbb{P}}(dy_i)$ is the density of Y_i (e.g., Merton, 1976).

Next, let $N_{i,t}$ be a Poisson process with a constant arrival rate of jumps λ_i and jump size Z_i, taking values $z_i \in \mathbb{R}$ for $i \in \{1, 2\}$. These processes are uncorrelated and specific to each asset. The idiosyncratic jump sizes are independently and identically normally distributed as $\mathcal{N}(\alpha_{ii}, \delta_{ii}^2)$. The expected proportional unique jump sizes are given by:

$$\kappa_{Z_i} = \mathbb{E}_{\mathbb{P}}[\exp(Z_i) - 1] = \int_{\mathbb{R}} [\exp(Z_i) - 1] m_{\mathbb{P}}(dz_i) \qquad i \in \{1, 2\},$$

where $m_{\mathbb{P}}(dz_i)$ is the density of Z_i.

In summary, for each asset, the n-th common jumps $Y_{1,n}$ and $Y_{2,n}$ occur simultaneously, determined by the same Poisson arrival process N_t. These jointly occurring jumps can be linked to macroeconomic shocks in the system, representing globally undiversifiable risks. The m-th jump $Z_{1,m}$ or k-th jump $Z_{2,k}$, specific to the i-th asset, is determined by the Poisson arrival process $N_{i,t}$. Jumps unique to each stock can be attributed solely to idiosyncratic shocks for that particular asset, defining globally diversifiable risks.

The return dynamics of the assets can be expressed as:

$$\begin{aligned}\frac{dX_i}{X_i} =& (\mu_i - \lambda\kappa_i - \lambda_i\kappa_{Z_i})dt + \sigma_i dW_{i,t} \\ &+ \int_{\mathbb{R}} [\exp(y_i) - 1] p(dy_i, dt) + \int_{\mathbb{R}} [\exp(z_i) - 1] p(dz_i, dt) \qquad i \in \{1, 2\},\end{aligned}$$

where $p(\cdot, dt)$ is the Poisson measure. Poisson measures and the bivariate Wiener process are independent. The stock prices are given by the solution:

$$S_{i,t} = S_{i,0} \exp\left(\big(\mu_i - \lambda\kappa_i - \lambda_i\kappa_{Z_i} - \frac{\sigma_i^2}{2}\big)t + \sigma W_{i,t} + \sum_{n=1}^{N_t} Y_{i,n} + \sum_{m=1}^{N_{i,t}} Z_{i,m} \right) \qquad i \in \{1, 2\}.$$

To achieve a suitable and fair evaluation of the final payoff conditioned on information about the underlying asset prices, the probability measure $\mathbb{P}$ is transformed to $\mathbb{Q}$ using the transformation proposed by Esscher (1932), see Appendix A.1. After applying the transformation, the change in the intensity is defined by:

$$\begin{aligned}\tilde{\lambda} &= \lambda\mathbb{E}_{\mathbb{P}}[\exp(\boldsymbol{\gamma}^T \boldsymbol{Y})] \\ \tilde{\lambda}_1 &= \lambda_1\mathbb{E}_{\mathbb{P}}[\exp(\beta_1 Z_1)] \\ \tilde{\lambda}_2 &= \lambda_2\mathbb{E}_{\mathbb{P}}[\exp(\beta_2 Z_2)],\end{aligned}$$

and the expected jump sizes are transformed to:

$$\begin{aligned}\tilde{\kappa}_i &= \mathbb{E}_{\mathbb{Q}}[\exp(Y_i) - 1] \qquad i \in \{1, 2\} \\ \tilde{\kappa}_{Z_i} &= \mathbb{E}_{\mathbb{Q}}[\exp(Z_i) - 1] \qquad i \in \{1, 2\}.\end{aligned}$$

Hence, under $\mathbb{Q}$, the distribution of the jump sizes also changes. Y_n remains independently and identically multivariate normally distributed with $\tilde{\boldsymbol{\alpha}} = \boldsymbol{\alpha} + \Sigma_{\boldsymbol{Y}}\boldsymbol{\gamma}$; the jump sizes Z_i are independently and identically normally distributed with $\tilde{\alpha}_{ii} = \alpha_{ii} + \delta_{ii}^2\beta_i$ for $i \in \{1, 2\}$.

The parameters $\boldsymbol{\gamma}$ for the joint process, and β_i with $i \in \{1,2\}$ for the distinct processes, are fundamental factors in the transition from $\mathbb{P}$ to $\mathbb{Q}$. The market, comprising assets with jump components, is inherently incomplete following the sense of Harrison and Pliska (1981). When accounting for market prices of jump risks, multiple equivalent martingale measures emerge, leading to different option prices. For example, if all factors equal zero, the scenario is akin to Merton (1976) where all jump risks are unpriced. If $\boldsymbol{\gamma} \neq \mathbf{0}$ and/or $\beta_i \neq 0$, changes occur in both jump-arrival intensities and jump-size distributions. Subsequently, in the empirical analysis attention is directed toward these parameters in the calibration process to establish the market premium for the defined risk classes, underscoring their key role in the model. It is also important to note that these parameters affect only the compounded Poisson processes, specifically the intensity and size of the jumps, without impacting the underlying risk itself. Therefore, these parameters are purely related to the tail risk.

For the derivation of a closed-form option pricing formula considering these factors, the money account is assumed as the numeraire (e.g., Geman et al., 1995). The resulting option price formula is based on the closed-form solution of Cheang and Chiarella (2011).[6] The dynamics under $\mathbb{Q}$ are expressed as:

$$\frac{X_i}{X_i} = r dt + \sigma_i d\tilde{W}_{i,t} + \int_{\mathbb{R}} [\exp(y_i) - 1] q(dy, dt) + \int_{\mathbb{R}} [\exp(z_i) - 1] q(dz_i, dt) \qquad i \in \{1,2\},$$

where $\tilde{W}_{i,t}$ denotes standard Brownian motion components under $\mathbb{Q}$, and q represents the Poisson measures under $\mathbb{Q}$. Therefore, the option price for the exchange of the two assets can be formulated as:

$$\begin{aligned} C(S_1,S_2) = \sum_k \sum_m \sum_n & \exp\big(-(\tilde{\lambda}_1 + \tilde{\lambda}_2 + \tilde{\lambda})(T-t)\big) \frac{(\tilde{\lambda}_1(T-t))^k}{k!} \frac{(\tilde{\lambda}_2(T-t))^m}{m!} \frac{(\tilde{\lambda}(T-t))^n}{n!} \\ & \times \Bigg[S_1 \exp\Big(-(\tilde{\lambda}_1 \tilde{\kappa}_{Z_1} + \tilde{\lambda}\tilde{\kappa}_1)(T-t) + k\tilde{\alpha}_{11} + \frac{k\delta_{11}^2}{2} + n\tilde{\alpha}_1 + \frac{n\delta_1^2}{2}\Big) \Phi(d_{1,t,k,m,n}) \\ & -S_2 \exp\Big(-(\tilde{\lambda}_2 \tilde{\kappa}_{Z_2} + \tilde{\lambda}\tilde{\kappa}_2)(T-t) + m\tilde{\alpha}_{22} + \frac{m\delta_{22}^2}{2} + n\tilde{\alpha}_2 + \frac{n\delta_2^2}{2}\Big) \Phi(d_{2,t,k,m,n}) \Bigg] \end{aligned}$$

where:

$$d_{1,t,k,m,n} = \frac{\ln(\frac{S_1}{S_2}) + (-\tilde{\lambda}(\tilde{\kappa}_1 - \tilde{\kappa}_2) - \tilde{\lambda}_1\tilde{\kappa}_{Z_1} + \tilde{\lambda}_2\tilde{\kappa}_{Z_2})(T-t) + \mu_{k,m,n} + \frac{\sigma_{k,m,n}^2(T-t)}{2}}{\sigma_{k,m,n}\sqrt{T-t}}$$

---

[6] Cheang and Chiarella (2011) defines the measure transformation using the Radon-Nikodym derivative, while this paper employs the Esscher transformation, more common in actuarial and option literature (e.g., Elliott et al., 2005). The Radon-Nikodym derivative provides separate parameters for jump probability and size, whereas the Esscher transformation defines a measure $\mathbb{Q}$ with a single parameter. The procedure for deriving the closed-form solution remains unaffected by these different approaches. Furthermore, it can be shown that the parameters of the Radon-Nikodym derivative have a unique relation to the parameter derived here, which also applies to further transformations such as the Wang transformation (e.g., Kijima, 2006; Labuschagne and Offwood, 2010). Therefore, the transformation selection is not a limitation here.

$$d_{2,t,k,m,n} = d_{1,t,k,m,n} - \sigma_{k,m,n}\sqrt{T-t},$$

with:

$$\mu_{k,m,n} = k(\tilde{\alpha}_{1,1} + \frac{\delta_{1,1}^2}{2}) - m(\tilde{\alpha}_{2,2} + \frac{\delta_{2,2}^2}{2}) + n(\tilde{\alpha}_1 - \tilde{\alpha}_2 + \frac{\delta^2}{2})$$

$$\sigma_{k,m,n}^2 = \sigma^2 + \frac{k\delta_{11}^2}{T-t} - \frac{m\delta_{22}^2}{T-t} + \frac{n\delta^2}{T-t},$$

where:

$$\delta^2 = \delta_1^2 + \delta_2^2 + \rho_Y \delta_1 \delta_2.$$

In the absence of jump risk, when $\tilde{\alpha}_i = \tilde{\alpha}_{ii} = 0$ and $\delta_i = \delta_{ii} = 0$, the jump intensity becomes zero, resulting in $\tilde{\kappa}_i = \tilde{\kappa}_{Z_i} = 0$ for $i \in \{1, 2\}$. Consequently, the option pricing formula of Margrabe (1978) is received, returning to the original model utilized at the beginning of the section. Given that this paper examines a single-period model, the subsequent content adheres to the condition of $T - t = 1$. This does not represent a limit but instead reflects non-life insurance contracts or cat bonds and cyber bonds, which are issued for a fixed term without adjustments during the period.

2.4 Alternative Models and Limits

To facilitate a comparison with the newly proposed OM, a standard model (SM) from expected value theory and an extension by Zanjani (2002) is presented. To maintain simplicity, no risk free discounting is applied. The premium is defined as the expected loss plus a loading:

$$P = (1 + \ell)\mathbb{E}[\bar{L}].$$

Estimating ℓ for insurance companies is challenging. To apply linear factor models to insurance seemed obvious, but direct estimation of liability betas is infeasible (e.g., Cummins and Harrington, 1985; Cox and Rudd, 1991). Therefore, these models are not suitable for understanding the high insurance prices, especially for catastrophic lines. Zanjani (2002) addressed this issue by proposing that the primary driver of catastrophe insurance prices is the cost of capital, rather than "beta" or other factors. He argues that while capital costs represent a relatively small portion of production costs in the broader industry, they are significant in lines like catastrophe insurance, which requires large amounts of supporting capital. Zanjani proposed an approach that integrates risk management with standard asset pricing, while also considering the policyholder's concern about solvency. According to Braun et al. (2023), the Zanjani model (ZM) can be summarized as follows:

$$P = \mathbb{E}[\bar{L}] - \mathbb{E}[D] + c.$$

Here, D denotes the difference between the expected payout and the realized payout in the event of insolvency:

$$D = max[\bar{L} - \bar{Y}_1, 0].$$

Since the default factor D also contains the premium, the model ZM does not have a closed-form solution. The cost of equity, denoted by c, is expressed as:

$$c = (\tau + r_{risk})S_0.$$

Here, r_{risk} signifies a risk premium determined by the correlation between loss and the capital market. This correlation is often assumed to be close to zero (e.g., Cummins and Harrington, 1985; Froot et al., 1995; Zanjani, 2002), which leads to frictional cost as the main driver. Amidst the Covid-19 crisis, scholars have begun to recalibrate this term. Currently, there is no definitive evidence regarding the specific nature of this factor. Suitable models for parameter estimation have yet to be established. Therefore, either factor models or consumption-based approaches are used (e.g., Braun et al., 2019a; Braun et al., 2019b).

Both alternative pricing models rely on first-order terms. In contrast, the new OM not only incorporates first-order terms but also identifies second-order terms as significant price drivers. Notably, terms related to the market environment are absent in the alternative models. While both models overlook market and loss uncertainties, the standard model also fails to consider any insolvency risks. Conversely, model ZM focuses solely on the insolvency risk for policyholders, without addressing the corresponding risk for shareholders.

All pricing models produce identical outcomes when jump risks, insolvency risks, and other frictions are removed. In such scenarios, the premium should correspond to the expected loss. This market is distinguished by either an infinite amount of equity or no variance. An equivalent scenario is a fully diversifiable risk, which is not priced, see Merton (1976).

Lemma 1. *Under the assumptions of a frictionless market without insolvency and jump risk, all models satisfy:*

$$\lim_{S_0 \to \infty} P = \mathbb{E}[\bar{L}] \text{ and } \lim_{\sigma \to 0} P = \mathbb{E}[\bar{L}].$$

Proof. See Appendix A.3. □

With Lemma 1 established, the models exhibit convergence in a frictionless market without insolvency and jump risks. Additionally, the OM demonstrates its capability to incorporate non-linear insolvency risks and jump risks into pricing within market contexts.

Lemma 2. *In a frictionless market without insolvency risk but with a positive probability of jump occurrences, the influence of jump risk is negligible, and consequently, it remains unpriced. The premium equals the expected loss:*

$$\lim_{S_0 \to \infty} P = \mathbb{E}[\bar{L}].$$

Proof. See Appendix A.3. □

With the ZM as defined here, the insurability of correlated jump risks is impossible in an insolvency-free market context. In the presence of correlated jump risks where $r_{risk} > 0$, it follows that if S_0 tends towards infinity, P also tends towards infinity. However, if the jumps can be assumed to be uncorrelated then $r_{risk} = 0$ and the ZM would also fulfill Lemma 2. This underlines the limits of a linear and constant factor approach when it comes to jump risks.

Besides the two alternative models presented here, there are also other possibilities. In the context of pricing cat bonds there exist contingent claim models that use compounded Poisson processes, such as models proposed by Lee and Yu (2002) or Ma and Ma (2013). However, the OM presented here differs in three key aspects: First, it is applicable across all four risk classes, not limited to cat bonds. Second, it provides a closed-form making it more practical and accessible. Third, it specifically prices the jump risk, rather than operating within the framework established by Merton (1976) with unpriced risk.

3 Application

To apply the OM, the model's parameters are estimated using historical data. It is important to emphasize that the purpose of this section is to apply the model and compare it with established models. The goal is to demonstrate how individual model parameters can be calibrated and to analyze their impact on pricing. This section does not aim for a precise real-world application, as this is not feasible given the limitations of the available data. For example, historical data on rare events are scarce, leading to a significant peso problem. Moreover, even when the dynamics of these events are known, the coverage signed may differ. As a result, the dynamics of the events and the loss portfolio can diverge significantly, for instance, when certain events are excluded from the coverage. A more detailed discussion on this point, along with a real-world application, is provided in Section4.

3.1 Calibration

For the risky rate $\bar{r}$ associated with the investment of the opening cash flows, the S&P 500 index is selected. The historical performance of the S&P 500 index, as reported by Morningstar (2023), shows an average annual total return of approximately 9% over the past decade, with a standard deviation of 15%. These parameters are applied to $\bar{r}$, meaning $\mathbb{E}[\bar{r}] = 0.09$ and $SD(1 + \bar{r}) = 0.15$. Unless otherwise specified, these are the baseline assumptions for the return.

The insurance sector demonstrated resilience during the financial crisis (OECD, 2011). Therefore, for the first two categories – locally insurable risk and globally insurable risk – no jump risks from the S&P 500 index are considered. However, for the last two categories, where the focus shifts to the presence of jump risks and the capital market, rather than insurers, covers the risks, this assumption no longer holds. For globally diversifiable risk, the jump of the risky rate is independent of the "insured" risk. Based on historical market shocks documented by MFS (2023), it is assumed that a market crash occurs every 10 years, with an average decline of 43.11% and a standard deviation of 0.34 times the expected value. This implies that $\lambda_1 = 0.1$, with the jump sizes given by $\mathbb{E}_{\mathbb{P}}[Z_1] = 0.5689$ and $SD(Z_1) = 0.34$. As discussed later, globally undiversifiable risk is estimated based on the occurrence of a pandemic. Historical data suggests that such events occur twice in a century (Centers for Disease Control and Prevention, 2023), with the assumption that a global pandemic triggers a capital market shock. Due to the limited data available to calibrate the jump sizes for such events, the previously estimated jump size is retained. However, the jump is now considered joint, with $\lambda = 0.02$.

The assessment of locally insurable risk relies on US indemnity losses, as documented in Frees and Valdez (1998). The dataset comprises 1,500 general liability claims, each representing indemnity payments in thousands of USD. The claims dataset is accessible through the R packages copula and evd. The expected loss per claim is 41.21 TUSD, with a standard deviation of 102.75 TUSD. The parameters are normalized to the expected loss without default risk, so $\mathbb{E}[L] = 1$ and $SD(L) = 2.45$.

Globally insurable risk is calibrated on data from Grinsted et al. (2019), encompassing the majority of United States hurricanes dating back to the early 20th century. For this risk category, extreme events are omitted, excluding the 10% of the most potent hurricanes (see Braun et al., 2023). Given the vulnerability of Texas and North Carolina to hurricanes and the absence of historical data indicating a hurricane simultaneously impacting both states (uncorrelated risk), these two states are used for the analysis. Following the data, Texas exhibits an expected annual hurricane loss of USD 1,685 million with a standard deviation 2.68 times the mean. North Carolina's expected annual hurricane loss amounts to USD 1,533 million with a standard deviation of 3.34 times the mean. The combined portfolio of hurricane losses for both states have an annual loss of USD 3,218 million with a standard deviation of 2.05 times the mean.

Globally diversifiable risk addresses the excluded 10% of the most potent hurricanes, which are now assumed to be transferred to the capital market via a cat bond. This means that the jump probability is 10%. All US hurricane losses from Grinsted et al. (2019) are taken into account. Typically, cat bonds have an attachment point beyond which they are triggered. In this context, the trigger is set at the 90% quantile of annual hurricane losses, meaning that only losses exceeding USD 64,503 million are covered. Losses below this threshold remain within the insurance market or are borne by policyholders. Consequently, the insurance market anticipates an expected annual hurricane loss of USD 15,966 million, with a standard deviation approximately 1.32 times the mean. The cat bond is assumed to cover losses up to a maximum of USD 103,373 million, corresponding to the 95% quantile. If a hurricane triggers the cat bond, an expected loss of USD 26,949 million falls into the capital market. This segment carries an expected annual hurricane loss with a standard deviation of around 0.53 times the expected value. After normalizing with respect to the loss that remains in the (re)insurance market, the expected jump size is $\mathbb{E}_{\mathbb{P}}[Z_2] = \frac{64{,}503+26{,}949}{15{,}966} = 5.7279$. It is also important to note that this calibration is not based on market-driven data from a traded bond. This is due to two key limitations: the availability of only annual data and the lack of information regarding the coverage, which will be adressed in detail in Section 4.

Globally undiversifiable risk is represented by a pandemic occurring twice per century, as evidenced by the Spanish flu and Covid-19 (Centers for Disease Control and Prevention, 2023). As there are only two data points for a pandemic to date, calibration is not possible.

Therefore, also to ensure comparability with cat bond from the globally diversifiable risk, the same jump size is assumed. This involves adopting a lower limit for the jump process, recognizing that, in reality, undiversifiable jumps are significantly larger (e.g., APICA, 2020). Consequently, the jump probabilities are reduced, but the jump itself is included as a joint process with correlated jump sizes. An overview of all components can be found in Table 1.

Risk category	$\mathbb{E}[\bar{r}]$	$SD(1+\bar{r})$	λ_1	$\mathbb{E}_{\mathbb{P}}[Z_1]$	$SD(Z_1)$	λ	$\mathbb{E}_{\mathbb{P}}[Y_1]$	$SD(Y_1)$
Locally insurable risk	0.09	0.15						
Globally insurable risk	0.09	0.15						
Globally diversifiable risk	0.09	0.15	0.1	0.5689	0.34			
Globally undiversifiable risk	0.09	0.15				0.02	0.5689	0.34
Risk category	$\mathbb{E}[\bar{L}]$	$SD(\bar{L})$	λ_2	$\mathbb{E}_{\mathbb{P}}[Z_2]$	$SD(Z_2)$	λ	$\mathbb{E}_{\mathbb{P}}[Y_2]$	$SD(Y_2)$
Locally insurable risk	1	2.45						
Globally insurable risk								
Texas	1	2.68						
North Carolina	1	3.34						
Mixed portfolio	1	2.05						
Globally diversifiable risk	1	1.32	0.1	5.729	0.53			
Globally undiversifiable risk	1	1.32				0.02	5.729	0.53

Table 1: Stochastic components of the OM.

This table summarizes all model parameters along with their variables and corresponding values. The upper section displays the calibration of the risk rate $\bar{r}$, while the lower section outlines the calibration of the loss $\bar{L}$, both of which depend on the respective risk categories.

To compare the OM with the ZM, r_{risk} must be estimated. Since general insurance-related betas are close to zero, $r_{risk} = 0$ holds for the first two categories. The latest estimate of $r_{risk} = 0.005$ for globally diversifiable risk and $r_{risk} = 0.206$ for globally undiversifiable risk from Braun et al. (2023) is used.

Frictional costs are assumed as follows: (1) $\tau = 0$ and (2) $\tau = 0.05$ for locally insurable risk, which, according to Zanjani (2002), corresponds to the commercial auto line. No frictional costs are assumed for globally insurable risk, as these are not necessary in the analysis. Braun et al.'s estimation for the cat bond market is also used for frictional costs and applies to both risk categories, as there is no calibration market for the latter category. Therefore $\tau = 0.045$ for both globally diversifiable risk and globally undiversifiable risk. Nevertheless, Zanjani (2002) has pointed out that the relative cost of capital varies with the underlying risk

3.2 Results

The results demonstrate that the OM can be applied across various risk categories and effectively prices risks in comparison to the existing ZM and SM models. It accounts for insolvency risks and diversification, highlighting the challenges that arise when large amounts of capital are required, driving up costs. Additionally, by taking the market environment into account, it can adapt to both soft and hard market phases. The OM determines market prices for cat bonds through a transformation of the measure, which is further explored in Section 4. Most importantly, the model underscores the limits of private risk sharing, showing that globally undiversifiable risks, such as pandemics, would incur such high transfer costs that they become economically unfeasible. This highlights the clear boundaries of private risk sharing and the necessity for public-private partnerships.

Locally Insurable Risk

Figure 1 provides an overview of the premium relative to the expected loss for models SM, ZM and OM, (a) without frictional costs and (b) with frictional costs of $\tau = \ell = 0.05$.

In the frictionless case, the premium in the SM remains fixed at 1, as expected, since insolvency risk and market conditions are not considered. The ZM consistently has the lowest premium because it reflects the policyholder's perspective, excluding shareholder risk. The OM falls between the other two models. These latter models align with the anticipated framework: as insolvency risk decreases, the premium rises, and both show the convergence towards the expected value, as outlined in Lemma 1. When frictional costs are introduced, the premium in the SM increases but stays constant. The relationship between models ZM and OM remains similar; however, due to the frictional costs, neither model converges to the expected value but instead experiences exponential growth. This exponential rise is driven by the large equity requirements, as the frictional costs are linear in equity, and the equity needed to cover 1% of the tail risk grows non-linearly, as described in Zanjani (2002).

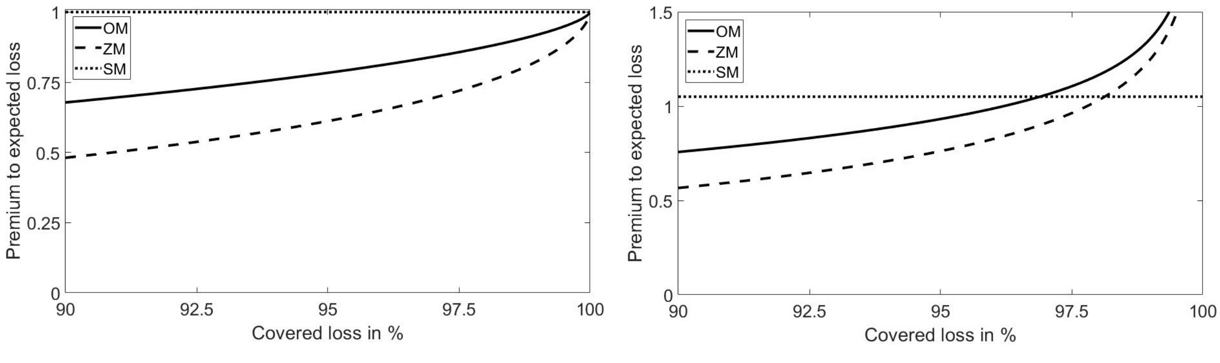

(a) Market with no frictonal costs.

(b) Market with $\tau = \ell = 0.05$.

Figure 1: Premium for different models and market scenarios.

This figure illustrates the premium relative to the expected loss for (a) a market without frictional costs and (b) a market with frictional costs of $\tau = \ell = 0.05$. It calculates the premium based on the coverage of the loss distribution for the SM, ZM, and OM.

Figure 2 illustrates the premium under (a) varying market volatilities and (b) different loss volatilities. As market volatility decreases, premiums rise because shareholders demand compensation for investing in safer equity, leading to higher premiums for policyholders seeking enhanced security. Conversely, when loss volatility decreases, the premium increases. This is due to the greater certainty and the convergence toward the expected loss. It is important to note that no frictional costs are included here. Higher volatility is often associated with the need to hold more capital, which in turn results in higher premiums.

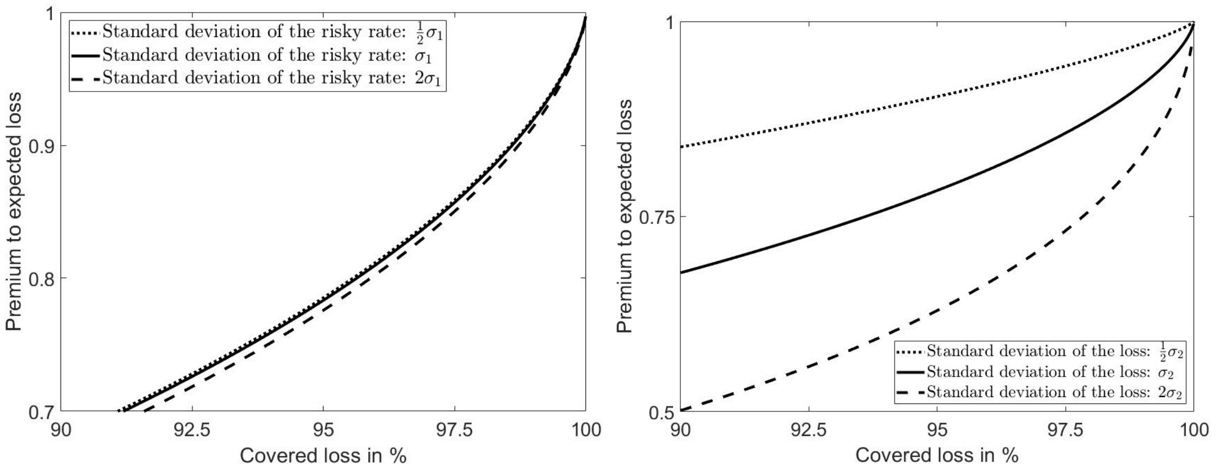

(a) Changing market volatility.

(b) Changing loss volatility.

Figure 2: Premium for different market and loss volatilities.

This figure illustrates the premium relative to the expected loss for (a) changing market volatilities and (b) changing loss volatilities. It calculates the premium based on the coverage of the loss distribution for the OM.

The model presented captures the price dynamics of locally insurable risks commonly observed in insurance markets. First, the assessment of default risk for policyholders is essential. Second, pricing mechanisms in these markets are significantly shaped by insolvency risk and frictional costs. Third, the premium is influenced by the dynamic interaction between market volatility, loss uncertainty, and insolvency risk. Consequently, the new OM not only addresses jump risks, as will be shown later, but also emphasizes the importance of incorporating higher-order factors to accurately reflect varying market conditions, such as soft or hard markets.

Globally Insurable Risk

Two separate hurricane risks are analyzed, one in Texas and the other in North Carolina. The data shows no common events in the past, indicating that these risks are uncorrelated. Two scenarios are compared: one where individual portfolios are insured locally, and another where a reinsurer covers the combined portfolio, diversifying the associated risks. Figure 3 illustrates the equity required for each (re)insurer to underwrite the risk. The reinsurer shows the highest capital requirement but also manages the largest policy volume. When comparing the aggregated capital needs of local insurers, the reinsurer consistently requires less capital for the same portfolio and insolvency risk, an effect that becomes more pronounced with increased tail risk. This is due to the global diversification achieved through reinsurance, highlighting a key benefit: the improved efficiency of risk diversification through a larger capital base. Figure 4 demonstrates this, as the reinsurer, by minimizing portfolio variance, can charge a lower risk premium, benefiting policyholders. However, this advantage diminishes when correlated events, like hurricanes affecting both Texas and North Carolina, occur.

The SM does not account for diversification (additive expected values), while the ZM incorporates this via the default variable D, as the default probability is tied to the cumulative distribution function. Additionally, like the OM, frictional costs decrease with reduced equity.

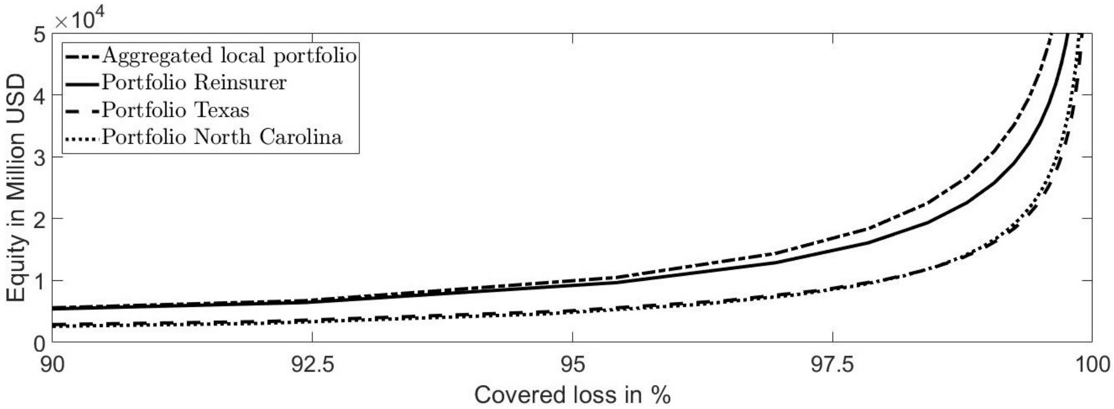

Figure 3: Equity for various local and global portfolios.

This figure illustrates the required equity for various portfolios: an aggregated portfolio comprising two local insurance portfolios that sum the losses from Texas and North Carolina; a reinsurer portfolio that diversifies the risks from both states; and the local portfolios addressing the risks from Texas and North Carolina individually. The equity is calculated based on the coverage of the loss distribution.

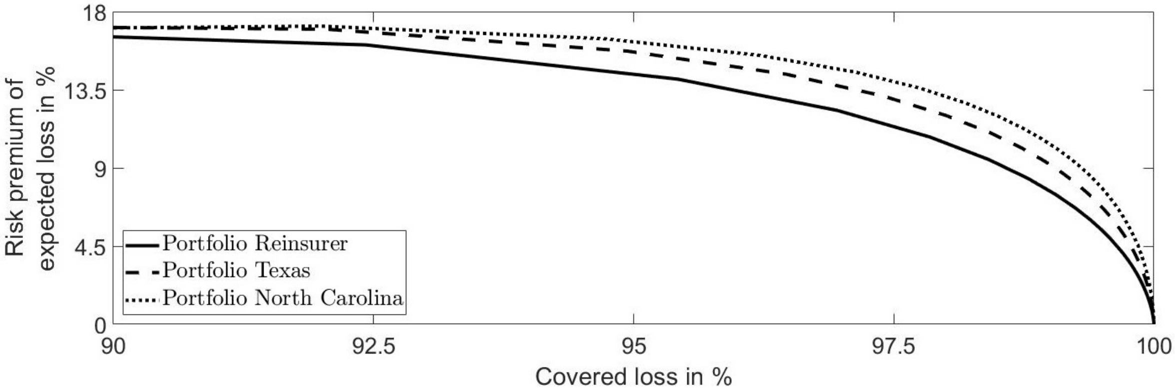

Figure 4: Risk premium for various local and global portfolios.

This figure illustrates the risk premium relative to the expected loss for three different portfolios: the local portfolios addressing the risks from Texas and North Carolina individually and a reinsurer portfolio that diversifies the risks from both states. It calculates the risk premium based on the coverage of the loss distribution.

Globally Diversifiable Risk

Three scenarios for the cat bond and the bond multiple – i.e., how many times the initial modeled expected loss investors receive in terms of the coupon – are examined (see Table 2). If the multiple equals 1, it indicates a coupon without a risk premium. A comparison with the SM is unnecessary here, as it does not include any of the dynamics and would be constant at 1. Furthermore, since catastrophe bonds are fully collateralized, meaning D in the ZM is zero, the ZM in this context reflects pricing based solely on traditional beta risk premiums. In Scenario 1, the probability of the jump in loss is positive, the risky rate has no jump risk, and there are no frictional costs. In this case, the multiple from the OM is approximately 1.07, indicating a risk premium of 7% of the expected loss. If the risky rate also has a risk of a crash, the risk premium falls to around 2%. It is consistent with previous results that the more volatile the market, the lower the premium. Scenarios 1 and 2 are identical in the ZM, as it does not include a market environment and has a multiple of 1.0766. This proximity to Scenario 1 of the OM is not coincidental. The estimated jump risks have comparatively low volatility (small second-order), there is no market environment taken into account, and both the market and the risk are uncorrelated, which emphasizes the relatively small r_{risk}. Accordingly, it is expected that both models estimate a small risk premium. Since the ZM cannot assess the jump risk in the risky rate, it overestimates the risk premium at this point. In the last scenario, frictional costs are added, and the risk premium rises to 58% for the OM and to 76% for the ZM. This aligns with previous research indicating that frictional costs account for a large part of the premium for extreme risks (e.g., Zanjani, 2002; Braun et al., 2023).

According to Artemis (2024b), the average multiple for the cat bond market for Q2 2024 is 4, meaning the risk premium is 300% of the expected loss. However, the market risk premium calculated here with the OM is only around 57%. Assuming that the underlying cat bond is priced consistently with the market, a probability distortion can be assumed. The parameters of the measure transformation must be calibrated accordingly. The calibration is straightforward. $\mathbb{Q}$ is determined via the transformation parameter, which corresponds to the market price. The ZM alone cannot estimate a measure transformation. Accordingly, another model would first have to be used to determine the measure $\mathbb{Q}$. For comparability, the measure transformation estimated with the OM is used here.

In Scenario 4, which has the same market conditions as Scenario 3, the ZM is unable to reflect the price accurately due to its reliance on a pure expected value structure, without accounting for jump risks and higher orders. In addition to the measure $\mathbb{Q}$, estimating the factor r_{risk} would also require a different approach, although the specifics are unknown. In the last scenario, Scenario 5, the frictional costs are removed for both models. A reduction in frictional costs can significantly reduce the risk premium, but it remains above the estimates with the $\mathbb{P}$ measure. Accordingly, the probability distortion of investors is another major cost driver next to frictional costs, which is uniquely estimated here using the market calibration.

		Estimates		Cat bond multiple	
Scenario	Measure	OM	ZM	OM	ZM
1	$\mathbb{P}$	$\lambda_2 = 0.1$	$r_{risk} = 0.005$	1.0689	1.0766
2	$\mathbb{P}$	$\lambda_1 = \lambda_2 = 0.1$	$r_{risk} = 0.005$	1.0201	1.0766
3	$\mathbb{P}$	$\lambda_1 = \lambda_2 = 0.1$ $\tau = 0.045$	$r_{risk} = 0.005$ $\tau = 0.045$	1.5783	1.7622
4	$\mathbb{Q}$	$\lambda_1 = \lambda_2 = 0.1$ $\tau = 0.045$ $\beta_2 = -0.402$	$r_{risk} = 0.005$ $\tau = 0.045$	4	2.5557
5	$\mathbb{Q}$	$\lambda_1 = \lambda_2 = 0.1$ $\beta_2 = -0.402$	$r_{risk} = 0.005$	2.8781	1.1556

Table 2: Multiples for the cat bond without and with measure transformation, estimated with the OM and ZM.

This table presents the results of cat bond pricing for both the OM and ZM. Five scenarios are analyzed: scenarios 1 to 3 are under the $\mathbb{P}$ measure, while scenarios 4 and 5 are based on the $\mathbb{Q}$ measure. Depending on the scenario, jump risks and frictional costs are considered. Details on what is included in the pricing can be found in the "estimates" tab for each respective model. The last two columns display the cat bond multiple derived for both models.

Globally Undiversifiable Risk

Table 3 displays the multiple for the pandemic bond. In Scenario 1, the joint jump is considered. Compared to the cat bond estimate, the multiple more than triples under the OM, despite the probability of occurrence being only one-fifth by the same jump size. Due to the linear risk cost assumption of the ZM and the high equity required, this model reaches a multiple of 16 under the $\mathbb{P}$ measure. Including frictional costs doubles the multiple for the OM and increases it by approximately 20% for the ZM. Although the tail risk – and consequently, ex-ante investor behavior – likely differs between pandemics and natural disasters, limited data necessitates the assumption that the probability distortion is identical to the estimated cat bond distortion. This assumption allows for a comparison of these risks. Scenario 3 demonstrates that the resulting market risk premium is more than 16 times the expected loss. For comparison, the largest historical market multiple was 7.5 at the inception of cat bonds in 2001 (Artemis, 2024b). When considering the $\mathbb{Q}$ measure for the ZM, the multiple exceeds 43. This leads to the conclusion that, given current market conditions, transferring pandemic risks through the capital market is not feasible (e.g., Gründl et al., 2021). Potential interventions could include reducing frictional costs. In Scenario 4, where no frictional costs are assumed, the multiple decreases to less than 11 for the OM and 35.5 for the ZM. While a market risk premium of just under 1000% of the expected loss remains very high, it represents a significant reduction. However, it is important to note that a lower limit for the jump size was used here. If the jump size increases, the relative multiple may remain stable, but the absolute values become unaffordable. Additionally, the correlation of jump sizes was omitted. Since only extreme events with comparably low variance that occur together due to the Poisson process are considered, correlation has minimal impact on the multiple here. However, it is evident that linear models and previous asset pricing models, such as the consumption model, are unsuitable for measuring this type of extreme risk due to the linear cost structure.

In conclusion, the pricing of a pandemic bond reveals that it is prohibitively expensive compared to other risk classes, making it difficult to transfer to the capital market without adjustments, such as government support (e.g., Braun et al., 2023). It is important to highlight that, to date, no instrument like a pandemic bond exists, and this analysis explains the reasons behind this absence.

		Estimates		Pandemic bond multiple	
Scenario	Measure	OM	ZM	OM	ZM
1	$\mathbb{P}$	$\lambda = 0.02$	$r_{risk} = 0.206$	3.8122	16.1562
2	$\mathbb{P}$	$\lambda = 0.02$ $\tau = 0.045$	$r_{risk} = 0.206$ $\tau = 0.045$	6.6439	19.4670
3	$\mathbb{Q}$	$\lambda = 0.02$ $\tau = 0.045$ $\gamma_2 = -0.402$	$r_{risk} = 0.206$ $\tau = 0.045$	17.2916	43.1152
4	$\mathbb{Q}$	$\lambda = 0.02$ $\gamma_2 = -0.4026$	$r_{risk} = 0.206$	10.8625	35.5646

Table 3: Multiples for a fictive pandemic bond without and with measure transformation, estimated with OM and ZM.

This table presents the results of fictional pandemic bond pricing for both the OM and ZM. Four scenarios are analyzed: scenarios 1 and 2 are under the $\mathbb{P}$ measure, while scenarios 3 and 4 are based on the $\mathbb{Q}$ measure. Depending on the scenario, frictional costs are considered. Details on what is included in the pricing can be found in the “estimates” tab for each respective model. The last two columns display the pandemic bond multiple derived for both models.

In summary, the new pricing model reflects the essential relationships between risk and the market, a component missing in previous models. It can calculate market premiums based on the market environment, accommodating both hard and soft market conditions. Additionally, it can price jump risks, whether independent or joint, which is challenging for previous models due to the lack of suitable factor models and sufficient data to estimate the risk of heavy-tailed distributions.

4 Real-World Estimation of $\mathbb{Q}$

The previous section aims to illustrate how individual model parameters can be calibrated and to assess their impact on pricing, without seeking a precise real-world application. A primary reason for this limitation is the insufficient data on natural catastrophic risks. In general, every cat bond is modeled by a specialized risk modeling and calculation agency. The modeling process does not rely solely on historical data but incorporates environmental factors such as climate change, expert opinions, and large-scale data simulations tailored to the structure of the underlying cat bond. For instance, cat bonds are written for specific risks, ranging from Asian property catastrophe risks to wildfire risks. Exclusions may also exist within the bonds; for example, many cat bonds for the "US named storm" risk type exclude Florida. Cat bonds also vary in terms of trigger type, attachment point, expected loss, and spread. Another challenge with using only historical data is the lack of transparency regarding the underlying coverage. Since the risk is initially underwritten by a (re)insurer or broker before being transferred to the capital market, it is essential to know which risks may have already been excluded, e.g., a coverage cap. For further details on cat bond structures, refer to Artemis (2024a).

This section aims to address the mentioned issues by using unique cyber data. The dataset is obtained from a leading risk modeling agent and based on a loss portfolio from a global reinsurer, which represents the worldwide cyber risk market. The dataset contains 10,000 losses, ranging from daily incidents to extreme events. Further details about the dataset are available in Kasper et al. (2024). The cyber bond market so far exhibits little heterogeneity in terms of risks. The trigger type is indemnity, and the risk type is cyber risks. Hannover Re's smaller 13.75 million Cumulus Re cyber bond, which focuses solely on cloud outages, is an outlier in this regard. An additional advantage is that cyber bonds have primarily been issued since December 2023, offering a short time span that allows for the comparison of investor risk attitudes within a single period. In the cat bond market, this risk attitude has proven to be time dependent, as shown in Artemis (2024b). Accordingly, the limitations mentioned before can be addressed and the peso problem can be avoided.

The analysis includes five market-traded cyber bonds from four different cedents, as shown in Table 4. Since January 2023, when Beazley issued the first cyber bond, five general cyber bonds have been issued by three more cedents. This analysis includes all cyber bonds for which the required information is publicly available (Artemis, 2024a). As a result, the analysis covers over 83% of the issued bonds and all cedents at least ones. This analysis encompasses over 6% of the total volume of new cat bond market transactions globally and nearly 8% of the transactions conducted during this period (AON, 2024). As outlined in Section 3.1, the stochastic components are calibrated based on the available data. However, the specific calibration results cannot be provided here due to the confidentiality of the data.[7]

---

[7] A key issue is that τ is currently unknown. Drawing a direct comparison to the cat bond market is inappropriate because the calibration of τ relies on models that are not suitable, as previously discussed, and frictional costs vary depending on the type of risk. Therefore, this analysis excludes all other cost drivers, such as τ and jumps in the risky rate, focusing instead of an upper bound for the cyber $\mathbb{Q}$. Since the other parameters influence the calibration for each bond in the same manner, this exclusion does not affect the overall results.

The uniqueness of this analysis cannot be overstated. First, the data from the risk modeling agency and the issued cyber bond come from a similar time frame, ensuring the risk assessment is up to date. Previous research has struggled to obtain such data, making this procurement a significant achievement. Second, the timing of this analysis aligns perfectly with the launch of the cyber bonds, meaning the bonds still reflect a relatively homogeneous risk. In contrast, the cat bond market, as well as the Cumulus Re cyber bond, show clear signs that the cyber bond market will become heterogeneous in the future, making such straightforward analysis possible only at this moment. Third, because of the understanding of the underlying cyber risk and the fact that the cyber bond exclusively covers pure tail risks, this analysis can identify a tail risk premium for the first time. In contrast, in stock or option markets, returns are influenced by various other factors.

Bond	Date of issue	Modeling agency	Cedent	Attachment point	Expected loss	Spread
1	Nov 2023	CyberCube	AXIS Capital	2.46%	1.97%	9.75%
2	Dec 2023	CyberCube	Swiss Re	2.228%	1.721%	12%
3	Dec 2023	CyberCube	Chubb	2.142%	1.387%	9.25%
4	Dec 2023	RMS	Beazley	1.71%	1.26%	13-13.25%
5	Sep 2024	RMS	Beazley	1.2%	0.93%	9.5-10.5%

Table 4: Public information of the target bonds.

This table presents public information on cyber bonds sourced from Artemis (2024a). For five bonds, it includes the date of issuance, the corresponding modeling agency, and the cedent. Additionally, bond-specific details such as the attachment point, the expected loss as a percentage of the notional amount, and the spread as a percentage of the notional amount are also provided.

Table 5 presents the calibration results, including the attachment and end quantile, the multiple, and the estimated β_2 for each bond. The results indicate that as the attachment quantile increases, the absolute value of β_2 also increases. The same applies to the relationship between the end quantile and β_2, but a higher multiple does not necessarily imply a higher β_2. To explore the relationship between β_2 and tail risk coverage, Figure 5 illustrates (a) the attachment quantile and (b) the end quantile in relation to β_2. Notably, there is a linear relationship between β_2 and the attachment quantile, while the relationship with the end quantile is less pronounced. This aligns with existing research, which suggests that catastrophe risk investors prioritize compensation for loss probability over loss severity (Braun et al., 2023; Braun et al., 2024). Furthermore, this calibration provides the first clear evidence that, besides an incomplete market, the measure $\mathbb{Q}$ is unique in relation to tail risk. This finding reinforces both the theoretical framework and the economic interpretation of investors' subjective ex-ante beliefs about tail risk, as described by Gao et al. (2019).

Bond	Attachment quantile	End quantile	Multiple	β_2
1	97.54%	99.583%	4.9492	-0.3805
2	97.772%	99.617%	6.9727	-0.5402
3	97.858%	99.697%	6.6691	-0.6020
4	98.29%	99.699%	10.3175 to 10.5159	-0.8230 to - 0.8293
5	98.8%	99.77%	10.2151 to 11.29	-0.9864 to -1.019

Table 5: Calibration output

This table provides calibration information for the five cyber bonds. It includes the attachment point and end quantile as percentages, along with the computed cyber bond multiple. The final column presents the estimated β_2, which represents the calibrated parameter of the $\mathbb{Q}$ measure.

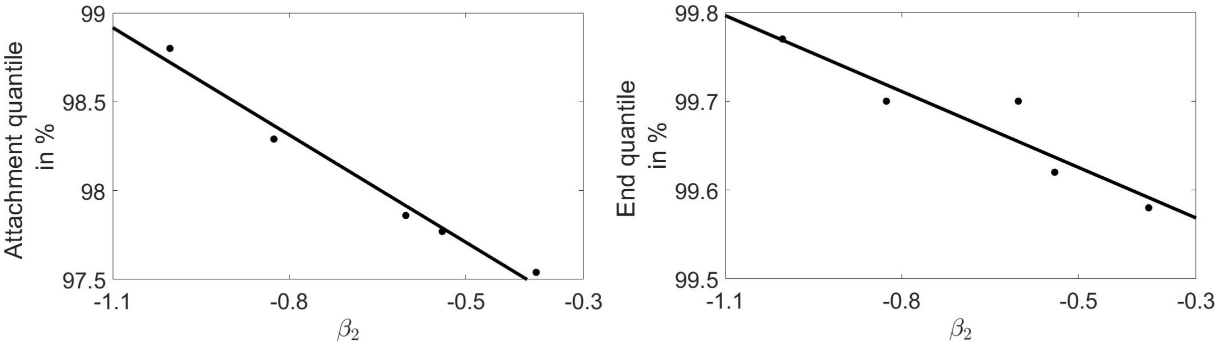

(a) Attachment quantile with $R^2 = 0.9793$.

(b) End quantile with $R^2 = 0.8792$.

Figure 5: Relationships with β_2.

This figure presents a scatter plot depicting the relationship between the estimated β_2 and (a) the attachment quantile, as well as (b) the end quantile. Additionally, it includes the optimal linear relationship represented by a trend line.

Economic interpretation

The results indicate that the higher the attachment point – meaning the lower the probability that the bond will be triggered – the higher the relative risk premium that investors expect. As previous studies have shown, this behavior cannot be explained by the relative risk aversion typically exhibited by investors in capital markets. Instead, the pricing behavior aligns more closely with prospect theory (Barberis, 2013). As Barberis and Huang (2008) demonstrate, prospect theory leads to a prediction that does not arise from traditional pricing models: specifically, that the skewness in the distribution of a security's returns – even idiosyncratic skewness unrelated to the overall market return – will be priced. In particular, a security with positively skewed returns will be overpriced relative to what would be expected in a traditional beta-risk-based economy. The variable $\mathbb{Q}$ in the model presented in this paper illustrates precisely this overpricing. Furthermore, the relationship between $\mathbb{Q}$ and the tail risk demonstrates that the relative overpricing increases as the risk in the tail grows. Importantly, this tendency is not inconsistent with observations in the insurance market. Sydnor (2010) shows that under probability weighting, households overweight tail events. As a result of their heightened focus on these unlikely but highly undesirable outcomes, households are willing to pay a higher premium for insurance policies. Since this study examines only traded bonds, it can be inferred that $\mathbb{Q}$ reflects the real-world equilibrium between the policyholder – who is willing to pay more for their insurance due to tail risk aversion – and the capital market investor, who shares this aversion, resulting in overpricing.

5 Discussion

5.1 The Catastrophic Markup Composition

According to Zanjani (2002), the main cause of high catastrophe markups in insurance pricing is the large capital commitment involved. Similarly, recent findings demonstrate that capital costs constitute a significant portion of the premium (Braun et al., 2023). Specifically, in the context of cat bonds, this commitment is particularly extreme due to the requirement for full collateralization. Moreover, factors such as the capital market cycle and the risk profile of the transaction play a crucial role, with diversification within the market being priced in (e.g.,Lane and Mahul, 2008; Herrmann and Hibbeln, 2023). However, empirical studies such as Braun et al. (2024) indicate that even after accounting for various factors, a substantial portion of the returns remains unexplained. This observation raises the question: What underlies these unexplained returns? The introduction of the measure $\mathbb{Q}$ as a probability distortion adds a solution to this discussion. Moreover, $\mathbb{Q}$ is assigned an economic significance that has traditionally been overlooked, as it has primarily been viewed as a "replication measure". As Borch (1960) noted, "we may need to sacrifice a principle deemed essential." While the proposed model is grounded in an equilibrium view of the world, it diverges from the assumption of frictionless, complete markets. Importantly, this divergence does not conflict with Zanjani's logic. By defining τ in Section 2 as the frictional component, the model effectively unifies different approaches to understanding these complex dynamics. Furthermore, it does not conflict with classical asset pricing betas. Assuming τ is defined not purely as friction but as $\tilde{\tau} = \tau + r_{risk}$ – where r_{risk}, as in Braun et al. (2023), is estimated using classical asset pricing models – the risk premium defined by $\mathbb{Q}$ is still needed (Barberis et al., 2021). So far, no classical beta can reflect the tail risk aversion of investors, which is not exclusive to the cat bond market but extends to others as well (Barberis and Huang, 2008). The idea of quantifying this aversion via the mass change in the jump can be extended to other markets and is future research. To summarize, this paper argues that a general composition of returns should consist of three components: frictional costs, traditional asset pricing, and an overpricing tail risk component, described by a probability distortion for tail risk, reflected by prospect theory.

5.2 Limitation and Future Research

A limitation of the OM is its assumptions regarding distributions. In traditional insurance practices, claims are often assumed to follow a lognormal distribution (e.g., Eling, 2012). Similarly, catastrophic pricing using compounded Poisson processes is a standard approach (e.g., Lee and Yu, 2002; Jaimungal and Wang, 2006). However, the distribution of jump risks remains uncertain. Many alternative models rely on expected value theory, assuming that "Peaks Over Threshold" (POT) events follow a generalized pareto distribution (GPD). The challenge with this approach is the lack of a universally accepted model for identifying POT events, the absence of a natural upper limit to POT losses, and the finite nature of moments in the GPD (McNeil et al., 2015). Moreover, insurance contracts and cat bonds introduce further complexity by capping payouts, which requires the use of truncated distributions. For example, Kasper et al. (2024) show that almost no "extreme tail" risk is covered in the cyber risk market. This raises the question of whether truncation even favors at the end the here chosen distributions as a potentially more suitable choice (e.g., Ma and Ma, 2013). This question presents an opportunity for future research. Additionally, an option model could be developed that better integrates extreme value theory and adjusts the distribution of jump risks within the GPD framework. Another potential enhancement could involve incorporating stochastic volatilities. However, given the small time frames involved and the availability of a closed-form solution for deterministic volatilities, this limitation appears to be acceptable.

A second direction for future research should focus on the measure $\mathbb{Q}$. This paper has already shown initial evidence that investors in the cyber bond market primarily define spreads based on concerns about tail risk. However, further analysis across various markets is needed to provide a clearer picture. A comparison between cat bonds and cyber bonds could also be insightful. This would require comparable data for both natural catastrophe events and cyber events, which could potentially be supplied by a risk modeling agency. The model presented in this paper can be used for such comparisons, as alternative models – such as those relying on time-series data – are not suitable due to the lack of extensive time-series data for cyber events. Moreover, it is essential to consider the time dimension of $\mathbb{Q}$. Historical data shows that cat bond multiples vary over time. This prompts the question of whether these changes are due to fluctuations in tail risk aversion or time-variant factors such as market risks, liquidity costs, seasonality, and other frictions (e.g., Lane and Mahul, 2008; Herrmann and Hibbeln, 2023). This leads to the follow-up question of the price setting. As previously mentioned, $\mathbb{Q}$ represents the equilibrium in the tail risk aversion between the policyholder and the capital market investor. However, a key distinction between cat bonds and cyber bonds to traditional investment instruments is that the investor most likely is also an policyholder. For example, he insures his private house against natural disasters or buys cyber insurance for his company. Therefore, it would be valuable to investigate who ultimately determines this price – whether it is the end customer (policyholder/investor) or an intermediary, such as a broker, which plays a central role in price setting (see the intermediary asset pricing literature).

6 Conclusion

This paper presents a novel and comprehensive model for pricing risk transfer instruments, offering a significant advancement in understanding how tail risks are transferred and priced across both insurance and capital markets. The model's unique integration of insurance / actuarial (e.g., Doherty and Garven (1986); Gerber and Shiu, 1994) and financial perspectives (e.g., Merton, 1976; Bates, 1996) addresses key limitations in traditional insurance methods, which often struggle with jump risks, correlation structures, and market frictions. A key contribution of this research is the transformation of the underlying jump process from $\mathbb{P}$ to $\mathbb{Q}$. This transformation is particularly impactful in cat bond and cyber bond markets, where tail risks are most prevalent. Through the application to cyber data, the paper offers one of the most precise calibrations to date, focusing on the emerging cyber bond market. The findings demonstrate that investors' concerns over tail risks primarily drive spreads. Even in incomplete markets, a unique $\mathbb{Q}$ can be defined, which Gao et al. (2019) describe as reflecting investors' subjective ex-ante beliefs driven by tail risk concerns. So far, traditional asset pricing models fall short describing this aversion (e.g., Braun et al., 2019a). Therefore, the finding has far-reaching implications for understanding market dynamics shaped by rare-event uncertainty and extreme aversion, which are also represented in the stock and options markets (e.g., Bollerslev and Todorov, 2011), and in line with previous findings of prospect theory (e.g., Barberis et al., 2001; Barberis and Huang, 2008).

This model offers a robust framework for assessing risk premiums in markets where traditional models lack explanatory power, highlighting a new driver of spreads – not just frictional costs and beta risk premiums but also tail risk aversion. This insight can help investors price securities more accurately and manage portfolios better in markets exposed to extreme risks. For governments and regulators, the model emphasizes the need for targeted financial market interventions for joint events, particularly in response to extreme severe risks like pandemics that threaten market stability. An example might include using the model to evaluate the risk exposure in public-private insurance schemes (Braun et al., 2023). Researchers will also benefit from this work, as it bridges the actuarial probability distortions and financial risk pricing, creating new approach for studying markets with significant jump risks and return compositions.

In sum, this model redefines the pricing landscape for insurance-linked securities by offering an empirically grounded, theoretically sound framework for navigating tail risks. It fills critical gaps in both the insurance and finance literature while delivering a practical and versatile tool for investors, policymakers, and researchers alike. Although derived primarily for cat bonds and cyber bond markets, the model's framework can be applied to any market exposed to jump risks, including stock, options or commodities, and other financial instruments where extreme events dominate pricing dynamics.

References

Ai, H. and Bhandari, A. (2021). Asset pricing with endogenously uninsurable tail risk. *Econometrica*, 89(3):1471–1505.

Andersen, T. G., Benzoni, L., and Lund, J. (2002). An empirical investigation of continuous-time equity return models. *The Journal of Finance*, 57(3):1239–1284.

Andersen, T. G., Fusari, N., and Todorov, V. (2020). The pricing of tail risk and the equity premium: Evidence from international option markets. *Journal of Business & Economic Statistics*, 38(3):662–678.

AON (2024). ILS Annual Report.

APICA (2020). APCIA Releases Update to Business Interruption Analysis.

Artemis (2024a). Catastrophe Bond & Insurance-Linked Securities Deal Directory. `https://www.artemis.bm/deal-directory`. [Online; accessed 25-July-2024.

Artemis (2024b). Catastrophe bonds and ILS average multiple by year. `https://www.artemis.bm/dashboard/cat_bonds_ils_average_multiple/`. [Online; accessed 09-February-2024].

Bai, J., Bali, T. G., and Wen, Q. (2019). Common risk factors in the cross-section of corporate bond returns. *Journal of Financial Economics*, 131(3):619–642.

Barberis, N. and Huang, M. (2008). Stocks as lotteries: The implications of probability weighting for security prices. *American Economic Review*, 98(5):2066–2100.

Barberis, N., Huang, M., and Santos, T. (2001). Prospect theory and asset prices. *The Quarterly Journal of Economics*, 116(1):1–53.

Barberis, N., Jin, L. J., and Wang, B. (2021). Prospect theory and stock market anomalies. *The Journal of Finance*, 76(5):2639–2687.

Barberis, N. C. (2013). Thirty years of prospect theory in economics: A review and assessment. *Journal of Economic Perspectives*, 27(1):173–196.

Bates, D. S. (1996). Jumps and stochastic volatility: Exchange rate processes implicit in deutsche mark options. *The Review of Financial Studies*, 9(1):69–107.

Black, F. and Scholes, M. (1973). The pricing of options and corporate liabilities. *Journal of Political Economy*, 81(3):637–654.

Bollerslev, T. and Todorov, V. (2011). Tails, fears, and risk premia. *The Journal of Finance*, 66(6):2165–2211.

Borch, K. (1960). The safety loading of reinsurance premiums. *Scandinavian Actuarial Journal*, 1960(3-4):163–184.

Bowers, N. L., Gerber, H. U., Hickman, J. C., Jones, D. A., and Nesbitt, C. (1986). *Actuarial Mathematics*. Itasca, Ill.: Society of Actuaries.

Braun, A., Ammar, S. B., and Eling, M. (2019a). Asset pricing and extreme event risk: Common factors in ils fund returns. *Journal of Banking & Finance*, 102:59–78.

Braun, A., Eling, M., and Freyschmidt, M. (2023). Optimal government intervention for extreme risks. *Available at SSRN*.

Braun, A., Herrmann, M., and Hibbeln, M. T. (2024). Common risk factors in the cross section of catastrophe bond returns. *Available at SSRN 3901695*.

Braun, A., Luca, D., and Schmeiser, H. (2019b). Consumption-based asset pricing in insurance markets: Yet another puzzle? *Journal of Risk and Insurance*, 86(3):629–661.

Caldana, R. and Fusai, G. (2013). A general closed-form spread option pricing formula. *Journal of Banking & Finance*, 37(12):4893–4906.

Centers for Disease Control and Prevention (2023). 100 years since 1918: Are we ready for the next pandemic?

Cheang, G. H. and Chiarella, C. (2011). Exchange options under jump-diffusion dynamics. *Applied Mathematical Finance*, 18(3):245–276.

Cox, L. A. and Rudd, E. A. (1991). Book versus market underwriting betas. *Journal of Risk and Insurance*, 58(2):312–321.

Cummins, J. D. (2006). Should the government provide insurance for catastrophes? *Federal Reserve Bank of St. Louis Review*, 88(4):337–379.

Cummins, J. D. and Harrington, S. (1985). Property-liability insurance rate regulation: Estimation of underwriting betas using quarterly profit data. *Journal of Risk and Insurance*, 52(1):16–43.

Cummins, J. D. and Weiss, M. A. (2009). Convergence of insurance and financial markets: Hybrid and securitized risk-transfer solutions. *Journal of Risk and Insurance*, 76(3):493–545.

De Roon, F. and Szymanowska, M. (2012). Asset pricing restrictions on predictability: Frictions matter. *Management Science*, 58(10):1916–1932.

Dickerson, A., Mueller, P., and Robotti, C. (2023). Priced risk in corporate bonds. *Journal of Financial Economics*, 150(2):103707.

Doherty, N. A. and Garven, J. R. (1986). Price regulation in property-liability insurance: A contingent-claims approach. *Journal of Finance*, 41(5):1031–1050.

Eling, M. (2012). Fitting insurance claims to skewed distributions: Are the skew-normal and skew-student good models? *Insurance: Mathematics and Economics*, 51(2):239–248.

Elliott, R. J., Chan, L., and Siu, T. K. (2005). Option pricing and esscher transform under regime switching. *Annals of Finance*, 1:423–432.

Eraker, B. (2004). Do stock prices and volatility jump? Reconciling evidence from spot and option prices. *The Journal of Finance*, 59(3):1367–1403.

Eraker, B., Johannes, M., and Polson, N. (2003). The impact of jumps in volatility and returns. *The Journal of Finance*, 58(3):1269–1300.

Esscher, F. (1932). On the probability function in the collective theory of risk. *Skandinavisk Aktuarietidskrift*, 15(3):175–195.

Frees, E. W. and Valdez, E. A. (1998). Understanding relationships using copulas. *North American Actuarial Journal*, 2(1):1–25.

Froot, K. A., Murphy, B., Stern, A., and Usher, S. (1995). The emerging asset class: Insurance risk. *Viewpoint*, 24(3). Originally ”Special Report from Guy Carpenter and Company, Inc.” July 1995.

Froot, K. A. and Stein, J. C. (1998). Risk management, capital budgeting, and capital structure policy for financial institutions: An integrated approach. *Journal of Financial Economics*, 47(1):55–82.

Gao, G. P., Lu, X., and Song, Z. (2019). Tail risk concerns everywhere. *Management Science*, 65(7):3111–3130.

Geman, H., El Karoui, N., and Rochet, J.-C. (1995). Changes of numeraire, changes of probability measure and option pricing. *Journal of Applied Probability*, 32(2):443–458.

Gerber, H. U. and Shiu, E. S. (1994). Option pricing by esscher transforms. *Transactions of Society of Actuaries*, 46:99–191.

Grinsted, A., Ditlevsen, P., and Christensen, J. H. (2019). Normalized US hurricane damage estimates using area of total destruction, 1900-2018. *Proceedings of the National Academy of Sciences*, 116(48):23942–23946.

Gründl, H., Guxha, D., Kartasheva, A., and Schmeiser, H. (2021). Insurability of pandemic risks. *Journal of Risk and Insurance*, 88(4):863–902.

Harrison, J. M. and Pliska, S. R. (1981). Martingales and stochastic integrals in the theory of continuous trading. *Stochastic Processes and their Applications*, 11(3):215–260.

Harvey, C. R. and Siddique, A. (2000). Conditional skewness in asset pricing tests. *The Journal of Finance*, 55(3):1263–1295.

Herrmann, M. and Hibbeln, M. (2023). Trading and liquidity in the catastrophe bond market. *Journal of Risk and Insurance*, 90(2):283–328.

Jaimungal, S. and Wang, T. (2006). Catastrophe options with stochastic interest rates and compound poisson losses. *Insurance: Mathematics and Economics*, 38(3):469–483.

Kasper, D., Freyschmidt, M., Cremer, F., and Grossklags, J. (2024). Cyber risk: (Re)insurance meets capital markets. *Working Paper*.

Kelly, B. and Jiang, H. (2014). Tail risk and asset prices. *The Review of Financial Studies*, 27(10):2841–2871.

Kijima, M. (2006). A multivariate extension of equilibrium pricing transforms: The multivariate esscher and wang transforms for pricing financial and insurance risks. *ASTIN Bulletin: The Journal of the IAA*, 36(1):269–283.

Kou, S. G. (2002). A jump-diffusion model for option pricing. *Management Science*, 48(8):1086–1101.

Labuschagne, C. C. and Offwood, T. M. (2010). A note on the connection between the esscher–girsanov transform and the wang transform. *Insurance: Mathematics and Economics*, 47(3):385–390.

Lane, M. and Mahul, O. (2008). Catastrophe risk pricing: An empirical analysis. *World Bank Policy Research Working Paper*, (4765).

Lee, J.-P. and Yu, M.-T. (2002). Pricing default-risky cat bonds with moral hazard and basis risk. *Journal of Risk and Insurance*, 69(1):25–44.

Luttmer, E. G. (1996). Asset pricing in economies with frictions. *Econometrica*, 64(6):1439–1467.

Ma, Z.-G. and Ma, C.-Q. (2013). Pricing catastrophe risk bonds: A mixed approximation method. *Insurance: Mathematics and Economics*, 52(2):243–254.

Margrabe, W. (1978). The value of an option to exchange one asset for another. *Journal of Finance*, 33(1):177–186.

McNeil, A. J., Frey, R., and Embrechts, P. (2015). *Quantitative risk management: Concepts, techniques and tools-Revised edition*. Princeton university press.

Merton, R. C. (1976). Option pricing when underlying stock returns are discontinuous. *Journal of Financial Economics*, 3(1-2):125–144.

MFS (2023). Market Declines: A History of Recoveries.

Morningstar (2023). S&P 500. `https://www.morningstar.com/indexes/spi/spx/risk`. [Online; accessed 12-December-2023].

OECD (2011). The Impact of the Financial Crisis on the Insurance Sector and Policy Responses.

Pan, J. (2002). The jump-risk premia implicit in options: Evidence from an integrated time-series study. *Journal of Financial Economics*, 63(1):3–50.

Ross, S. (2023). A History of the S&P 500 Dividend Yield. `https://www.investopedia.com/articles/markets/071616/history-sp-500-dividend-yield.asp`. [Online; accessed 01-February-2024].

Rubinstein, M. (1976). The valuation of uncertain income streams and the pricing of options. *The Bell Journal of Economics*, 7(2):407–425.

Runggaldier, W. J. (2003). Jump-diffusion models. In *Handbook of heavy tailed distributions in finance*, pages 169–209. Elsevier.

Sydnor, J. (2010). (Over)insuring modest risks. *American Economic Journal: Applied Economics*, 2(4):177–199.

Wang, S. S. (2000). A class of distortion operators for pricing financial and insurance risks. *Journal of Risk and Insurance*, 67(1):15–36.

Zanjani, G. (2002). Pricing and capital allocation in catastrophe insurance. *Journal of Financial Economics*, 65(2):283–305.

A Appendix

A.1 Measure Changes using the Esscher Transformation

Define an asset as:

$$S_t = S_0 \exp(X_t),$$

where $X_t t \geq 0$ is a stochastic process characterized by stationary and independent increments, and $X_0 = 0$. Furthermore, let:

$$F_{X_t}(x) = \mathbb{P}(X_t \leq x)$$

be the cumulative distribution function, and:

$$M_{\mathbb{P},X_t}(u) = \mathbb{E}[\exp(uX_t)]$$

represent the moment-generating function of the random variable X_t under the measure $\mathbb{P}$. Thus:

$$M_{\mathbb{P},X_t}(u) = \int_{-\infty}^{\infty} \exp(ux) f(x,t) dx,$$

where $f(x,t)$ is the continuous density of X_t.[8] Building upon the transformation proposed by Esscher (1932), a transformed density for X_t is:

$$\begin{aligned} f(x,t,h) &= \frac{\exp(hx)f(x,t)}{\int_{-\infty}^{\infty} \exp(hy) f(y,t) dy} \\ &= \frac{\exp(hx)f(x,t)}{M_{\mathbb{P},X_t}(h)} \end{aligned}$$

where h is the transformation parameter. The corresponding moment-generating function is given by:

$$\begin{aligned} M_{Q,X_t}(u) &= \int_{-\infty}^{\infty} \exp(ux) f(x,t,h) dx \\ &= \frac{M_{\mathbb{P},X_t}(u+h)}{M_{\mathbb{P},X_t}(u)}. \end{aligned}$$

Subsequently, the Esscher transformation is derived for the three significant processes in this study. The analytical findings align with prior literature, exemplified by works such as Gerber and Shiu (1994) and Runggaldier (2003), where, for instance, Runggaldier transforms these measures utilizing the Radon-Nikodym theorem. In the provided examples, the time component is disregarded, as it is not needed in this context.

---

[8] For a discrete distribution, the integral can be replaced by a sum.

Normal Distribution: Assuming $X_t = Y_t$, where Y_t is a normally distributed random variable with a mean of μ and a variance of σ^2. The moment-generating function is expressed as:

$$M_{\mathbb{P},X_t}(u) = \exp(u\mu + \frac{1}{2}\sigma^2 u^2).$$

Through the Esscher transformation, the resulting expression for the moment-generating function under the new measure $\mathbb{Q}$ is:

$$M_{\mathbb{Q},X_t}(u) = \exp\Big(u(\mu + h\sigma^2) + \frac{1}{2}\sigma^2 u^2\Big).$$

Consequently, the new mean under $\mathbb{Q}$ can be defined as $\tilde{\mu} = \mu + h\sigma^2$. The transformed normal distribution under $\mathbb{Q}$ remains a normal distribution with mean $\tilde{\mu}$ variance σ^2.

Proof.

$$\begin{aligned}
\frac{M_{\mathbb{P},X_t}(u+h)}{M_{\mathbb{P},X_t}(u)} &= \frac{\exp\big((u+h)\mu + \frac{1}{2}\sigma^2(u+h)^2\big)}{\exp(u\mu + \frac{1}{2}\sigma^2 u^2)} \\
&= \exp\Big((u+h)\mu + \frac{1}{2}\sigma^2(u+h)^2 - (u\mu + \frac{1}{2}\sigma^2 u^2)\Big) \\
&= \exp\Big((h\mu + \frac{1}{2}\sigma^2 h^2 + \sigma^2 uh\Big) \\
&= \exp\Big((h(\mu + \sigma^2 u) + \frac{1}{2}\sigma^2 h^2\Big)
\end{aligned}$$

□

Poisson Distribution: Assume $X_t = kN_t$, where N_t is a Poisson process with intensity λ, and k is a constant. The moment-generating function is defined as:

$$M_{\mathbb{P},X_t}(u) = \exp\Big(\lambda(\exp(ku) - 1)\Big)$$

Through the Esscher transformation, the resulting expression for the moment-generating function under the new measure $\mathbb{Q}$ is:

$$M_{\mathbb{Q},X_t}(u) = \exp\Big(\lambda\exp(hk)(\exp(ku) - 1)\Big)$$

Consequently, the intensity under $\mathbb{Q}$ can be defined as $\tilde{\lambda} = \lambda\exp(hk)$. The transformed Poisson process under $\mathbb{Q}$ remains a Poisson process with intensity $\tilde{\lambda}$.

Proof.

$$\begin{aligned}
\frac{M_{\mathbb{P},X_t}(u+h)}{M_{\mathbb{P},X_t}(u)} &= \frac{\exp\big(\lambda(\exp(k(u+h)) - 1)\big)}{\exp\big(\lambda(\exp(ku) - 1)\big)} \\
&= \exp\Big(\lambda(\exp(k(u+h)) - 1) - \lambda(\exp(ku) - 1)\Big) \\
&= \exp\Big(\lambda(\exp(ku)\exp(kh)) - \lambda\exp(ku)\Big) \\
&= \exp\Big(\lambda\exp(ku)(\exp(kh) - 1)\Big)
\end{aligned}$$

□

Compounded Poisson Process: Assume a compounded Poisson process $X_t = \sum_{i=1}^{N_t} Y_t$, where N_t is a Poisson process with intensity λ, and Y_t represents a normally distributed jump size with mean μ and variance σ^2. The moment-generating function is defined as:

$$\begin{aligned} M_{\mathbb{P},X_t}(u) &= \mathbb{E}[\exp(u\sum_{i=1}^{N_t} Y_i)] \\ &= \exp\big(\lambda(M_{\mathbb{P},Y_t}(u) - 1)\big) \end{aligned}$$

Through the Esscher transformation, the resulting expression for the moment-generating function under the new measure $\mathbb{Q}$ is:

$$M_{\mathbb{Q},X_t}(u) = \exp\Big(\lambda M_{\mathbb{P},Y_t}(h)(M_{\mathbb{Q},Y_t}(u) - 1)\Big)$$

Consequently, the intensity under $\mathbb{Q}$ can be defined as $\tilde{\lambda} = \lambda M_{\mathbb{P},Y_t}(h)$, and the new mean of the jump size under $\mathbb{Q}$ can be defined as $\tilde{\mu} = \mu + h\sigma^2$. The transformed compounded Poisson process under $\mathbb{Q}$ remains a compounded Poisson process with intensity $\tilde{\lambda}$ and mean jump size $\tilde{\mu}$ and variance σ^2.

Proof.

$$\begin{aligned} \frac{M_{\mathbb{P},X_t}(u+h)}{M_{\mathbb{P},X_t}(u)} &= \frac{\exp\big(\lambda(M_{\mathbb{P},Y_t}(u+h) - 1)\big)}{\exp\big(\lambda(M_{\mathbb{P},Y_t}(u) - 1)\big)} \\ &= \exp\Big(\lambda(M_{\mathbb{P},Y_t}(u+h) - 1) - \lambda(M_{\mathbb{P},Y_t}(u) - 1)\Big) \end{aligned}$$

Given the moment-generating function of a normally distributed random variable, one obtains:

$$\begin{aligned} M_{\mathbb{P},Y_t}(u+h) &= \exp\Big((u+h)\mu + \frac{1}{2}\sigma^2(u+h)^2\Big) \\ &= \exp\Big(u\mu + h\mu + \frac{1}{2}\sigma^2u^2 + \frac{1}{2}\sigma^2h^2 + \sigma^2uh\Big) \\ &= \exp\Big(u\mu + \frac{1}{2}\sigma^2u^2 + h(\mu + \sigma^2u) + \frac{1}{2}\sigma^2h^2\Big) \\ &= M_{\mathbb{P},Y_t}(u)M_{\mathbb{Q},Y_t}(h) \end{aligned}$$

Therefore:

$$\begin{aligned} \frac{M_{\mathbb{P},X_t}(u+h)}{M_{\mathbb{P},X_t}(u)} &= \exp\Big(\lambda(M_{\mathbb{P},Y_t}(u)M_{\mathbb{Q},Y_t}(h) - 1) - \lambda(M_{\mathbb{P},Y_t}(u) - 1)\Big) \\ &= \exp\Big(\lambda M_{\mathbb{P},Y_t}(u)M_{\mathbb{Q},Y_t}(h) - \lambda M_{\mathbb{P},Y_t}(u)\Big) \\ &= \exp\Big(\lambda M_{\mathbb{P},Y_t}(u)(M_{\mathbb{Q},Y_t}(h) - 1)\Big) \end{aligned}$$

□

A.2 Influence of Dividends on Premiums

Following Cheang and Chiarella (2011), both assets may yield a dividend return denoted as $\xi_i, i \in \{1,2\}$. In the context of this study, wherein S_2 represents the loss, dividend payments do not apply to this asset, resulting in $\xi_1 \geq 0$ and $\xi_2 = 0$. Consequently, the formulation of the option price for the exchange of the two assets, accounting for dividends, can be formulated as:

$$
\begin{aligned}
C(S_1,S_2) = \sum_k \sum_m \sum_n \exp\big(-(\tilde{\lambda}_1+\tilde{\lambda}_2+\tilde{\lambda})\big)\frac{(\tilde{\lambda}_1)^k}{k!}\frac{(\tilde{\lambda}_2)^m}{m!}\frac{(\tilde{\lambda})^n}{n!} \\
\times\Bigg[S_1 \exp\Big(-(\xi_1+\tilde{\lambda}_1\tilde{\kappa}_{Z_1}+\tilde{\lambda}\tilde{\kappa}_1)+k\tilde{\alpha}_{11}+\frac{k\delta_{11}^2}{2}+n\tilde{\alpha}_1+\frac{n\delta_1^2}{2}\Big)\Phi(d_{1,t,k,m,n}) \\
-S_2 \exp\Big(-(\tilde{\lambda}_2\tilde{\kappa}_{Z_2}+\tilde{\lambda}\tilde{\kappa}_2)+m\tilde{\alpha}_{22}+\frac{m\delta_{22}^2}{2}+n\tilde{\alpha}_2+\frac{n\delta_2^2}{2}\Big)\Phi(d_{2,t,k,m,n})\Bigg]
\end{aligned}
$$

where:

$$
d_{1,t,k,m,n} = \frac{\ln(\frac{S_1}{S_2})+(-\tilde{\lambda}(\tilde{\kappa}_1-\tilde{\kappa}_2)-\tilde{\lambda}_1\tilde{\kappa}_{Z_1}+\tilde{\lambda}_2\tilde{\kappa}_{Z_2}-\xi_1)+\mu_{k,m,n}+\frac{\sigma_{k,m,n}^2}{2}}{\sigma_{k,m,n}\sqrt{T-t}}.
$$

The other terms remain unchanged.

Given the indemnity losses in the US from the example in Section 3.1. The dividend yield of the S&P 500 index was at the end of 2022 by 1.78%, whereas historical dividend yields for the S&P 500 index have typically ranged from between 3% to 5% (Ross, 2023). Figure 6 illustrates the premium differences between dividends and no dividends. The pattern resembles that seen with frictional costs. This suggests that dividends in alternative investments are a price determinant for insurance contract premiums.

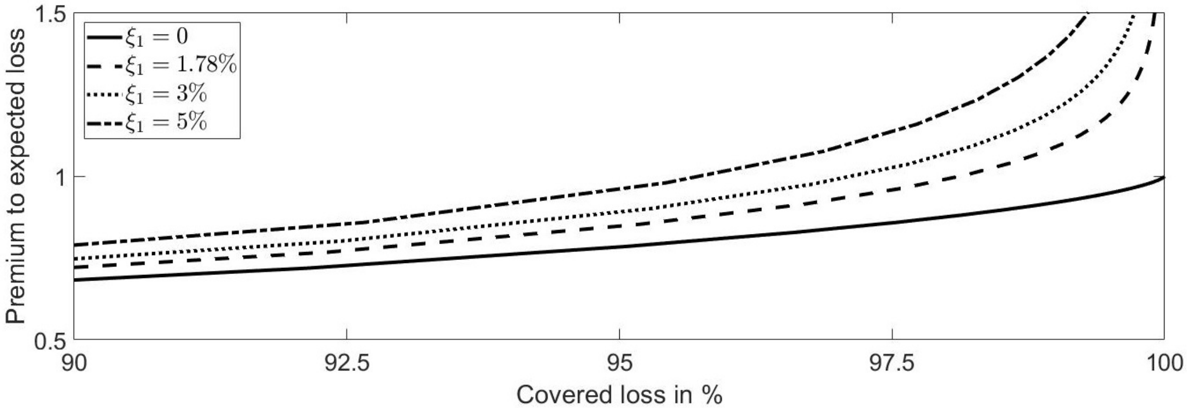

Figure 6: Premium for different dividends.

This figure illustrates the premium relative to the expected loss for four different dividends. It calculates the premium based on the coverage of the loss distribution.

A.3 Proofs

Lemma 1

Proof. In the standard model, the proof is straightforward. In the extension, given the absence of insolvency risk, $E[D] = 0$. Moreover, without friction and jump risk, $c = 0$. Hence, $P = \mathbb{E}[\bar{L}]$. In the option model, when jump risk is absent, the following relationships hold:

$$\begin{aligned} && Y_0\Phi(d_1) - \mathbb{E}[\bar{L}]\Phi(d_2) =& S_0 \\ \Leftrightarrow && (S_0 + P)\Phi(d_1) - \mathbb{E}[\bar{L}]\Phi(d_2) =& S_0 \\ \Leftrightarrow && S_0(\Phi(d_1) - 1) + P\Phi(d_1) - \mathbb{E}[\bar{L}]\Phi(d_2) =& 0 \end{aligned}$$

It is observed that:

$$\lim_{S_0\to\infty} d_1 = \lim_{\sigma\to 0} d_1 = \infty \quad \text{and} \quad \lim_{S_0\to\infty} d_2 = \lim_{\sigma\to 0} d_2 = \infty,$$

leading to:

$$\lim_{S_0\to\infty} \Phi(d_1) = \lim_{\sigma\to 0} \Phi(d_1) = 1 \quad \text{and} \quad \lim_{S_0\to\infty} \Phi(d_2) = \lim_{\sigma\to 0} \Phi(d_2) = 1.$$

Consequently, the equation simplifies to:

$$\begin{aligned} && S_0(\Phi(d_1) - 1) + P\Phi(d_1) - \mathbb{E}[\bar{L}]\Phi(d_2) =& 0 \\ \Leftrightarrow && P - \mathbb{E}[\bar{L}] =& 0 \\ \Leftrightarrow && P =& \mathbb{E}[\bar{L}] \end{aligned}$$

□

Lemma 2

Proof. In the scenario where $\sigma \to 0$, uncertainty diminishes, eliminating jump risks. Consequently, the focus lies solely on the case where $S_0 \to \infty$. Without loss of generality, k, m and n can be fixed:

$$\begin{gathered} \exp\big(-(\tilde{\lambda}_1 + \tilde{\lambda}_2 + \tilde{\lambda})\big)\frac{(\tilde{\lambda}_1)^k}{k!}\frac{(\tilde{\lambda}_2)^m}{m!}\frac{(\tilde{\lambda})^n}{n!} \\ = \\ \exp\big(-\tilde{\lambda}_1\big)\frac{(\tilde{\lambda}_1)^k}{k!}\exp\big(-\tilde{\lambda}_2\big)\frac{(\tilde{\lambda}_2)^m}{m!}\exp\big(-\tilde{\lambda}\big)\frac{(\tilde{\lambda})^n}{n!} \\ = \\ \mathbb{P}_{\tilde{\lambda}_1}(k)\mathbb{P}_{\tilde{\lambda}_2}(m)\mathbb{P}_{\tilde{\lambda}}(n), \end{gathered}$$

given the Poisson distribution of the jump occurrences. From the previous proof it is known that for $S_0 \to \infty$:

$$\Phi(d_1, t, k, m, n) = \Phi(d_2, t, k, m, n) = 1.$$

Thus, the option formula can be expressed as:

$$\begin{aligned}C(Y_1(P),\bar{L}) =&\sum_k\sum_m\sum_n \mathbb{P}_{\tilde{\lambda}_1}(k)\mathbb{P}_{\tilde{\lambda}_2}(m)\mathbb{P}_{\tilde{\lambda}}(n)\\ &\times\Bigg[Y_0\exp\Big(-(\tilde{\lambda}_1\tilde{\kappa}_{Z_1}+\tilde{\lambda}\tilde{\kappa}_1)+k\tilde{\alpha}_{11}+\frac{k\delta_{11}^2}{2}+n\tilde{\alpha}_1+\frac{n\delta_1^2}{2}\Big)\\ &-\mathbb{E}[\bar{L}]\exp\Big(-(\tilde{\lambda}_2\tilde{\kappa}_{Z_2}+\tilde{\lambda}\tilde{\kappa}_2)+m\tilde{\alpha}_{22}+\frac{m\delta_{22}^2}{2}+n\tilde{\alpha}_2+\frac{n\delta_2^2}{2}\Big)\Bigg]\end{aligned}$$

Moreover:

$$\begin{aligned}\exp(k\tilde{\alpha}_{11}+\frac{k\delta_{11}^2}{2}) &= \mathbb{E}[\exp(kZ_1]\\ \exp(m\tilde{\alpha}_{22}+\frac{m\delta_{22}^2}{2}) &= \mathbb{E}[\exp(mZ_2)]\\ \exp(n\tilde{\alpha}_1+\frac{n\delta_1^2}{2}) &= \mathbb{E}[\exp(nY_1)]\\ \exp(n\tilde{\alpha}_2+\frac{n\delta_2^2}{2}) &= \mathbb{E}[\exp(nY_2)],\end{aligned}$$

and defining $\sum_{k,m,n}\mathbb{P}_{\tilde{\lambda}_1,\tilde{\lambda}_2,\tilde{\lambda}}(k,m,n)=\sum_k\sum_m\sum_n\mathbb{P}_{\tilde{\lambda}_1}(k)\mathbb{P}_{\tilde{\lambda}_2}(m)\mathbb{P}_{\tilde{\lambda}}(n)$:

$$\begin{aligned}C(Y_1(P),\bar{L}) =&\sum_{k,m,n}\mathbb{P}_{\tilde{\lambda}_1,\tilde{\lambda}_2,\tilde{\lambda}}(k,m,n)\Bigg[Y_0\exp\Big(-(\tilde{\lambda}_1\tilde{\kappa}_{Z_1}+\tilde{\lambda}\tilde{\kappa}_1)\Big)\mathbb{E}[\exp(kZ_1)]\mathbb{E}[\exp(nY_1)]\\ &-\mathbb{E}[\bar{L}]\exp\Big(-(\tilde{\lambda}_2\tilde{\kappa}_{Z_2}+\tilde{\lambda}\tilde{\kappa}_2)\Big)\mathbb{E}[\exp(mZ_2)]\mathbb{E}[\exp(nY_2)]\Bigg]\\ =&\Bigg[Y_0\exp\Big(-(\tilde{\lambda}_1\tilde{\kappa}_{Z_1}+\tilde{\lambda}\tilde{\kappa}_1)\Big)\sum_{k,m,n}\mathbb{P}_{\tilde{\lambda}_1,\tilde{\lambda}_2,\tilde{\lambda}}(k,m,n)\mathbb{E}[\exp(kZ_1)]\mathbb{E}[\exp(nY_1)]\\ &-\mathbb{E}[\bar{L}]\exp\Big(-(\tilde{\lambda}_2\tilde{\kappa}_{Z_2}+\tilde{\lambda}\tilde{\kappa}_2)\Big)\sum_{k,m,n}\mathbb{P}_{\tilde{\lambda}_1,\tilde{\lambda}_2,\tilde{\lambda}}(k,m,n)\mathbb{E}[\exp(mZ_2)]\mathbb{E}[\exp(nY_2)]\Bigg]\end{aligned}$$

The call option must equate to the initial equity, therefore:

$$\begin{aligned}C(Y_1(P),\bar{L}) =&(S_0+P)\exp\Big(-(\tilde{\lambda}_1\tilde{\kappa}_{Z_1}+\tilde{\lambda}\tilde{\kappa}_1)\Big)\sum_{k,m,n}\mathbb{P}_{\tilde{\lambda}_1,\tilde{\lambda}_2,\tilde{\lambda}}(k,m,n)\mathbb{E}[\exp(kZ_1)]\mathbb{E}[\exp(nY_1)]\\ &-\mathbb{E}[\bar{L}]\exp\Big(-(\tilde{\lambda}_2\tilde{\kappa}_{Z_2}+\tilde{\lambda}\tilde{\kappa}_2)\Big)\sum_{k,m,n}\mathbb{P}_{\tilde{\lambda}_1,\tilde{\lambda}_2,\tilde{\lambda}}(k,m,n)\mathbb{E}[\exp(mZ_2)]\mathbb{E}[\exp(nY_2)]\\ =&S_0.\end{aligned}$$

For the sake of a simpler overview, let's define:

$$J_1=\sum_{k,m,n}\mathbb{P}_{\tilde{\lambda}_1,\tilde{\lambda}_2,\tilde{\lambda}}(k,m,n)\mathbb{E}[\exp(kZ_1)]\mathbb{E}[\exp(nY_1)]$$

and:

$$J_2 = \sum_{k,m,n} \mathbb{P}_{\tilde{\lambda}_1,\tilde{\lambda}_2,\tilde{\lambda}}(k,m,n)\mathbb{E}[\exp(mZ_2)]\mathbb{E}[\exp(nY_2)]$$

as a placeholder. Isolating the premium yields to:

$$\begin{aligned}
P =&\mathbb{E}[\bar{L}]\frac{\exp\Big(-(\tilde{\lambda}_2\tilde{\kappa}_{Z_2}+\tilde{\lambda}\tilde{\kappa}_2)\Big)J_2}{\exp\Big(-(\tilde{\lambda}_1\tilde{\kappa}_{Z_1}+\tilde{\lambda}\tilde{\kappa}_1)\Big)J_1} + S_0\frac{1-\exp\Big(-(\tilde{\lambda}_1\tilde{\kappa}_{Z_1}+\tilde{\lambda}\tilde{\kappa}_1)\Big)J_1}{\exp\Big(-(\tilde{\lambda}_1\tilde{\kappa}_{Z_1}+\tilde{\lambda}\tilde{\kappa}_1)\Big)J_1}\\
=&\mathbb{E}[\bar{L}]\exp\Big(-(\tilde{\lambda}_2\tilde{\kappa}_{Z_2}-\tilde{\lambda}_1\tilde{\kappa}_{Z_1}+\tilde{\lambda}(\tilde{\kappa}_2-\tilde{\kappa}_1))\Big)\frac{J_2}{J_1} + S_0\frac{1-\exp\Big(-(\tilde{\lambda}_1\tilde{\kappa}_{Z_1}+\tilde{\lambda}\tilde{\kappa}_1)\Big)J_1}{\exp\Big(-(\tilde{\lambda}_1\tilde{\kappa}_{Z_1}+\tilde{\lambda}\tilde{\kappa}_1)\Big)J_1}
\end{aligned}$$

Upon closer examination of J_1, its expression can be rephrased. Without loss of generality, the same restructuring applies to J_2 by substituting k and m:

$$\begin{aligned}
J_1 &= \sum_{k,m,n} \mathbb{P}_{\tilde{\lambda}_1,\tilde{\lambda}_2,\tilde{\lambda}}(k,m,n)\mathbb{E}[\exp(kZ_1)]\mathbb{E}[\exp(nY_1)]\\
&= \underbrace{\sum_m \mathbb{P}_{\tilde{\lambda}_2}(m)}_{=1}\sum_k \mathbb{P}_{\tilde{\lambda}_1}(k)\mathbb{E}[\exp(kZ_1)]\sum_n \mathbb{P}_{\tilde{\lambda}}(n)\mathbb{E}[\exp(nY_1)].
\end{aligned}$$

Without loss of generality, the focus remains on $\sum_k \mathbb{P}_{\tilde{\lambda}_1}(k)\mathbb{E}[\exp(kZ_1)]$ with this equivalence extending to other components sharing a similar structure:

$$\begin{aligned}
\sum_k \mathbb{P}_{\tilde{\lambda}_1}(k)\mathbb{E}[\exp(kZ_1)] &= \sum_k \mathbb{P}_{\tilde{\lambda}_1}(k)\exp(k\tilde{\alpha}_{11}+k\frac{\delta_{22}^2}{2})\\
&= \sum_k \mathbb{P}_{\tilde{\lambda}_1}(k)\exp(\tilde{\alpha}_{11}+\frac{\delta_{22}^2}{2})^k\\
&= \sum_k \mathbb{P}_{\tilde{\lambda}_1}(k)\mathbb{E}[\exp(Z_1)]^k\\
&= \sum_k \mathbb{P}_{\tilde{\lambda}_1}(k)\exp\big(k\ln(\mathbb{E}[\exp(Z_1)])\big)
\end{aligned}$$

Reflecting on the fact that the moment-generating function of a Poisson-distributed random variable x is defined as $M_X(u) = \mathbb{E}[\exp(uX)] = \sum_n \mathbb{P}(X=n)\exp(un)$, this results in:

$$\begin{aligned}
\sum_k \mathbb{P}_{\tilde{\lambda}_1}(k)\exp\big(k\ln(\mathbb{E}[\exp(Z_1)])\big) &= M_{N_1}\big(ln(M_{Z_1})\big)\\
&= \exp(\tilde{\lambda}_1(\exp\big(\ln(\mathbb{E}[\exp(Z_1)])\big)-1))\\
&= \exp(\tilde{\lambda}_1\underbrace{\big(\mathbb{E}[\exp(Z_1)]-1\big)}_{\tilde{\kappa}_{Z1}})\\
&= \exp(\tilde{\lambda}_1\tilde{\kappa}_{Z1}).
\end{aligned}$$

Summarized, it holds:

$$\begin{aligned} J_1 &= \exp(\tilde{\lambda}_1 \tilde{\kappa}_{Z1}) \exp(\tilde{\lambda} \tilde{\kappa}_1) \\ J_2 &= \exp(\tilde{\lambda}_2 \tilde{\kappa}_{Z2}) \exp(\tilde{\lambda} \tilde{\kappa}_2) \end{aligned}$$

Therefore, the following applies to the premium:

$$\begin{aligned} P =& \mathbb{E}[\bar{L}] \exp\Big(-(\tilde{\lambda}_2 \tilde{\kappa}_{Z_2} - \tilde{\lambda}_1 \tilde{\kappa}_{Z_1} + \tilde{\lambda}(\tilde{\kappa}_2 - \tilde{\kappa}_1))\Big) \frac{\exp(\tilde{\lambda}_2 \tilde{\kappa}_{Z2}) \exp(\tilde{\lambda} \tilde{\kappa}_2)}{\exp(\tilde{\lambda}_1 \tilde{\kappa}_{Z1}) \exp(\tilde{\lambda} \tilde{\kappa}_1)} \\ &+ S_0 \frac{1 - \exp\Big(-(\tilde{\lambda}_1 \tilde{\kappa}_{Z_1} + \tilde{\lambda} \tilde{\kappa}_1)\Big) \exp(\tilde{\lambda}_1 \tilde{\kappa}_{Z1}) \exp(\tilde{\lambda} \tilde{\kappa}_1)}{\exp\Big(-(\tilde{\lambda}_1 \tilde{\kappa}_{Z_1} + \tilde{\lambda} \tilde{\kappa}_1)\Big) \exp(\tilde{\lambda}_1 \tilde{\kappa}_{Z1}) \exp(\tilde{\lambda} \tilde{\kappa}_1)} \\ =& \mathbb{E}[\bar{L}] \exp\Big(-(\tilde{\lambda}_2 \tilde{\kappa}_{Z_2} - \tilde{\lambda}_1 \tilde{\kappa}_{Z_1} + \tilde{\lambda}(\tilde{\kappa}_2 - \tilde{\kappa}_1))\Big) \exp\Big((\tilde{\lambda}_2 \tilde{\kappa}_{Z_2} - \tilde{\lambda}_1 \tilde{\kappa}_{Z_1} + \tilde{\lambda}(\tilde{\kappa}_2 - \tilde{\kappa}_1))\Big) \\ &+ S_0 \frac{1 - \exp\Big(-(\tilde{\lambda}_1 \tilde{\kappa}_{Z_1} + \tilde{\lambda} \tilde{\kappa}_1)\Big) \exp(\tilde{\lambda}_1 \tilde{\kappa}_{Z1} + \tilde{\lambda} \tilde{\kappa}_1)}{\exp\Big(-(\tilde{\lambda}_1 \tilde{\kappa}_{Z_1} + \tilde{\lambda} \tilde{\kappa}_1)\Big) \exp(\tilde{\lambda}_1 \tilde{\kappa}_{Z1} + \tilde{\lambda} \tilde{\kappa}_1)} \\ =& \mathbb{E}[\bar{L}] \end{aligned}$$

$\square$